Rheological context of emplacement of the Dori, Gorom-Gorom and Touka Bayèl granitic plutons (northeast Burkina Faso, West African Craton)

Adama Ouédraogo Yaméogo, Pascal Ouiya, Abraham Seydoux Traoré, Saga Sawadogo, Séta Naba, Sonia Rousse, Mélina Macouin

Journal Pre-proof

Rheological context of emplacement of the Dori, Gorom-Gorom and Touka Bayèl granitic plutons (northeast Burkina Faso, West African Craton)

Adama Ouédraogo Yameogo, Pascal Ouiya, Abraham Seydoux Traore, Saga Sawadogo, Séta Naba, Sonia Rousse, Mélina Macouin

PII: S1464-343X(23)00254-6

DOI: https://doi.org/10.1016/j.jafrearsci.2023.105081

Reference: AES 105081

To appear in: *Journal of African Earth Sciences*

Received Date: 19 June 2023

Revised Date: 18 September 2023

Accepted Date: 2 October 2023

Please cite this article as: Yameogo, Adama.Oué., Ouiya, P., Traore, A.S., Sawadogo, S., Naba, Sé., Rousse, S., Macouin, Mé., Rheological context of emplacement of the Dori, Gorom-Gorom and Touka Bayèl granitic plutons (northeast Burkina Faso, West African Craton), *Journal of African Earth Sciences* (2023), doi: https://doi.org/10.1016/j.jafrearsci.2023.105081.

Rheological context of emplacement of the Dori, Gorom-Gorom and Touka Bayèl granitic plutons (northeast Burkina Faso, West African Craton)

Authors: **Adama Ouédraogo YAMEOGO[a*,b], Pascal OUIYA[b,c], Abraham Seydoux TRAORE[b], Saga SAWADOGO[b], Séta NABA[b], Sonia ROUSSE[d], Mélina MACOUIN[d]**

[a] *: Université Norbert ZONGO, Département des Sciences de la Vie et de la Terre, Unité de Formation et de Recherche en Sciences et Technologies, BP 376 Koudougou, Burkina Faso*

[b] *: Laboratoire Géosciences et Environnement (LaGE), Université Joseph KI-ZERBO, Département des sciences de la Terre, Unité de Formation et de Recherche en Sciences de la Vie et de la Terre, 03 BP 7021 Ouaga 03, Burkina Faso*

[c] *: Ecole Normale Supérieure (ENS)/Institut Sciences et Technologies (IST), 01 BP 1757 Ouaga 01, Burkina Faso*

[d] *: Laboratoire Géosciences Environnement Toulouse UMR 5563 & UR 234 IRD, Université Paul Sabatier, Avenue Edouard Belin 14, 31400 Toulouse, France.*

* **Correspondances**: **Adama Ouédraogo YAMEOGO[a*,b]**: ayameogofr@yahoo.fr, Téléphone : +22672473292

Abstract

The reconstitution of the geodynamic processes of the Eburnean orogeny in the time span around 2.1 Ga in Dori area is here carried out through the examination of the internal structures and microstructures of the Dori, Gorom-Gorom and Touka Bayèl granitic plutons. The radiometric ages of these plutons vary between 2164 Ma and 2148 Ma. The internal structures have been evidenced using the Anisotropy of Magnetic Susceptibility (AMS) method and the examination of microstructures through thin sections under optical microscope.

The organization of the internal fabrics strongly suggests a diapiric emplacement for the Dori and the Touka Bayèl plutons in a still soften crust. The pluton of Gorom-Gorom seems to be constituted of four small plutons. Three of them, coalescent in the southern part, are emplaced by the diapirism and the fourth in the northern part can be interpreted as emplaced in a tension gash.

The overall disposition of the fabrics lets suggest a synchronous emplacement in accordance with the dextral sense of the Tiébélé-Dori-Markoye (TDM) shear zone in a regional E-W shortening context responsible of a crustal thickening.

The two emplacement mechanisms (diapirism and tension gash) identified through the internal fabrics testify a rheological contrast of the crust during this early period of the Eburnean Orogeny.

Key words: Burkina Faso, Paleoprotrozoic/Eburnean, Plutons, magnetic fabrics, microstructures, rheology

1. Introduction

The paleoproterozoic domain of the Man/Léo shield in the southern part of the West African Craton is constituted of more or less narrow greenstones belts crosscut by granitoids' plutons during the Eburnean orogeny. The magmatic and orogenic accretion processes seem to spread out with some diachronism in this domain also called the Baoulé-Mossi domain (Grenholm et al., 2019). The reconstitution of the geodynamic processes that prevailed during the Eburnean orogeny and priorly is a subject of debate (Doumbia et al., 1998; Vidal et al., 2009; Lompo, 2010; Wane et al., 2018; Grenholm et al., 2019; Chardon et al., 2020; Traoré et al., 2022).

In all cases, the radiometric ages and the isotopic signatures of rocks confirm the juvenile character of the Paleoproterozoic/birimian crust (Abouchami et al., 1990; Boher et al., 1992 Liégeois et al., 1991; Taylor et al., 1992; Doumbia et al., 1998; Gasquet et al., 2003; Pawlig et al., 2006; Tapsoba et al., 2013; Para-Avila et al., 2016; Eglinger et al., 2017; Mériaud et al., 2020). However, some segments of reworked pre-birimian crusts have been mentioned in the centre of Côte d'Ivoire and in Ghana and are probably related to the genesis of certain granitoids (Gasquet et al., 2003; Block et al., 2016; Petersson et al., 2016).

Granitoids are known to occupy an important volume in the Baoulé-Mossi domain. This justifies the numerous studies with the aim to carry out their petrologic and geochemical characters (Hirdes et al., 1996; Doumbia et al., 1998; Egal et al., 2002; Pawlig et al., 2006; Tapsoba et al., 2013; Eglinger et al., 2017; Yaméogo et al., 2020). Granitoids are known to be good markers of the crustal deformation and following this argument, other studies have been focused on the characterization of the internal fabrics (foliations, lineations) in order to reconstitute their emplacement mechanisms (Pons et al., 1992; Pons et al., 1995; Lompo et

al., 1995; Vidal et al., 1996; Naba et al., 2004; Vegas et al., 2008; Traoré et al., 2011; Sawadogo et al., 2018).

Since it is known that granitoids with the same geochemical characteristics can be emplaced in different geodynamic contexts (Nédelec and Bouchez, 2011), highlighting the internal structures of plutons is the best alternative to characterize the context at the time of their emplacement.

The present study deal with the rheological context and emplacement mechanisms of the Dori, Gorom-Gorom and Touka Bayèl granitic plutons (Fig. 1), through the analysis of internal structures and microstructures. These granitoids, according to Tshibubudze et al. (2015), were emplaced between 2164 and 2148 Ma, and are prior to the local D1 phase of the Eburnean Orogeny.

The Baoulé-Mossi domain is known for his huge potential of gold mineralization and so the majority of geological studies were first focused on the relationships between the gold mineralization and the main phases of deformation of the Eburnean orogeny (Milesi et al., 1991; Feybesse et al., 2006; Baratoux et al., 2015; Amponsah et al., 2016; Ouiya et al., 2016; Tshibubudze and Hein, 2016; Woodman et al., 2016; Sawadogo et al., 2018 and references therein). In many cases, gold mineralization occurs after the first phase of deformation namely D1 (Milesi et al., 1989; Feybesse et al., 2006; Grenholm et al., 2019 and references therein). Thus, the characterization of geodynamic context of the Baoulé-Mossi domain in term of deformation during the period prior to the D1 event haven't been sufficiently discussed by the previous studies. The recent radiometric ages on the rocks from the Oudalan-Gorouol belt and the neighboring granitoids (Tshibubudze et al., 2015) shows that the emplacement age of the Dori batholith is prior to D1 event in this locality.

The aim of the present study is to use the measurements of the Anisotropy of Magnetic Susceptibility coupled with the microstructures examinations in order established the geodynamical context of emplacement of these plutons and so participate to well characterized the style of deformation during the period which preceded D1 or Tangaean event after Hein, 2010 and Tshibubudze et al. (2013).

2. Regional geological setting

The studied area is located in the northeastern part of Burkina Faso in the Man/Leo shield (Fig. 2). In accordance with main lithologies of the Man/Leo shield, the studied area is constituted of granitoid that intruded metavolcanic and metasedimentary rocks. The metavolcanic and metasedimentary rocks constitute what is traditionally called Birimian greenstones belts and metasedimentary basins (Hirdes et al., 1996; Baratoux et al., 2011). The metavolcanics rocks with various natures are mainly metabasalts, metaandesits, metadacites, metarhydodacites and metarhyolites (Castaing et al., 2003; Lompo, 2010; Tapsoba et al., 2013). In the metasedimentary basins, the main rocks are shales, metapelites, metagreywackes with some intercalations of calk-alkaline metavolcanics rocks (Hirdes et al., 1996; Béziat et al., 2000 and references therein).

For the lithostratigraphic succession of the birimian series, it is now established that the bottom is occupied by the dominant métavolcanic unit while, the top is constituted by the dominant metasedimentary unit. The birimian series are overlain by the sediments from Tarkwaian group (Perrouty et al., 2012, Tshibubudze et al., 2015; Wane et al., 2018 and references therein).

Regarding to the geodynamical context of emplacement of the volcanic units some of the authors (Sylvester and Attoh, 1992; Ama Salah et al., 1996; Beziat et al., 2000; Soumaila et al., 2004; Dampare et al., 2008) propose an environment similar to those of present island arcs while the others (Abouchami et al., 1990; Boher et al., 1992; Pouclet et al., 1996; Lompo, 2009) propose an environment of oceanic plateaus with active mantle plumes.

The birimian greenstones belts and metasedimentary basins are crosscut by plutons of granitoids with various natures.

The emplacement of the granitoids is spread over a time interval of 68 Ma (2165 Ma to 2097 Ma) during the Eburnean Orogeny (Hirdes et al., 1996; Doumbia et al., 1998; Castaing et al., 2003; Tapsoba et al., 2013; Tshibubudze et al., 2013; Tshibubudze et al., 2015). According to Castaing et al. (2003); Naba et al. (2004); Yaméogo et al. (2020), two generations of granitoids have been distinguished. The first generation has some affinities with Archean TTG. At field scale, these granitoids are commonly foliated with iron-bearing silicates such as amphibole and biotite. The second generation is composed of apparently isotropic calc-akaline to alkaline granitoid that content, according to Naba et al. (2004), only biotite as iron-bearing silicates.

As describe at many places in the Man/Leo shield, the Eburnean orogeny is characterized by regional metamorphism into the greenschist facies (Castaing et al., 2003; Feybesse et al., 2006; Baratoux et al., 2011 and references therein). Locally, the amphibolite facies is mentioned at

the contact of certain plutons (Debat et al., 2003; Soumaila et Garba, 2006) or along shear zones (Chevremont et al., 2003). Using chemical analysis data on minerals and thermodynamic models, Ganne et al. (2011) have shown that minerals such as chlorite and phengite from Paleoproterozoic rocks of eastern Burkina Faso, Western Niger and the Kédougou-Kéniéba inlier were formed at high pressures of 10–12 kbar, low temperatures of 400–450°C and under a geothermal gradient of 10–12°C km^{-1} and therefore are the marks of a modern-style plate tectonics at this period.

Regarding the phases of deformations, the three main phases defined by Milési et al. (1989); Feybesse et Milési (1994) and Feybesse et al. (2006) for the Eburnean orogeny, seem to not be representative for the whole Baoulé-Mossi domain. A synthesis of available data from the whole domain (Grenholm et al., 2019) shows that the orientations of the stresses, the ages and the styles of deformation vary from one area to another.

In the northern region of Burkina Faso, Hein (2010) defined for the Goren belt the first phase of deformation (D1) also called Tangaean event characterized by NE-SW compression which is responsible of folding, reverse-dextral shear zones with NW to NNW trends and a penetrative schistosity.

In the Oudalan-Gorouol belt, Tshibubudze et al. (2015) described the Tangaean event as responsible of formation of certain branches of the Markoye shear zone. Western more, in the Djibo belt, McCuaig et al. (2016) describe the D1 phase NNE-SSW oriented as responsible of ESE fabric which is correlable with the Tangaean event of Hein (2010).

The Dori and Gorom-Gorom plutons, respectively of about 1092 km^2 and 1200 km^2, are composed of biotite granite. The small pluton of Touka Bayèl, located south of the Gorom-Gorom pluton with the same composition as the latter, seems to be an apophysis.

Through the petrographic and geochemical characterization of the Dori and Gorom-Gorom plutons, Yameogo et al. (2020) shown that they have the same characters concerning their macroscopic habitus and their majors, traces and rare earth elements contents. They are metalumineous to peralumineous and highly potassic. According to the geotectonic diagrams, the Dori and Gorom-Gorom plutons were emplaced in an active tectonic context which has the same characteristic with nowadays subduction zones. The transcurrent shearing which controls gold mineralization in the area (case of Essakane deposit) took place later after the emplacement of these plutons.

Airborne geophysical data (BUMIGEB, 2015) and particularly the image of the analytical signal of the total magnetic intensity shaded at 45° NW of the study area (Fig. 3) allow to specify the cartographic limits of the plutons (Touka Bayèl, Dori and Gorom-Gorom). The same image also allows to interpret all the major shears zones, faults and dykes that run through the study area. Thus, between the Gorom-Gorom and Dori plutons, some of these major shear zones, showing NNE-SSW to NE-SW orientation, are branches of the Tiébélé-Dori-Markoye (TDM) shear zone also locally call the Markoye shear zone.

Some structures less longer than the major shear zone with mean NE strike seem to be precocious and are largely disturbed (folded) near the northern contact of the Dori pluton. This disturbance is probably due to the thermal effect related to emplacement of this pluton (Fig. 3). Late doleritic dykes, NW-SE oriented (Baratoux et al., 2019), that crosscut all petrographic units are underlined by yellow on the Fig. 3.

3. Methodology

The fabric of the granitoids here studied was highlighted by measurements of the Anisotropy of Magnetic Susceptibility (AMS) parameters. For these measurements, core sampling was carried out using a portable drilling machine following a grid of 2 km x 2 km. On each sampling station, at least, two cores with fifth to ten centimetres in length and spaced two to ten meters are drilled. A total of 448 sampling stations have been performed in this study: 282 stations in granitic plutons (145 stations in Dori pluton, 136 stations in Gorom-Gorom pluton and 34 stations in Touka Bayèl pluton) and 133 stations in the country rocks. The sampling stations in the country rocks have been performed near the limits of the plutons in order to appreciate the geometrical relationships between pluton internal fabrics and those of the TTG basement. In the laboratory, each core is cut into at least two samples of approximately spherical shape (diameter ≈ 25 mm and height ≈ 22 mm) for measurements of the AMS. For a station, at least, four samples are subject to AMS measurements in order to prove statistically the consistency of the mean values calculated in all cases. The rest of the core is used for thin section for microstructure studies.

The AMS measurements were performed in the Laboratoire Géosciences et Environnement de Toulouse (GET) using a susceptometer Kappabridge KLY-3-Agico operating under a weak alternating field of 4×10^{-4} T, at a frequency of 920 Hz with a sensitivity of about 5×10^{-8} SI. These measurements allow to access scalar and directional data of AMS ellipsoid. The three

axis of the ellipsoid namely K1≥ K2≥ K3 are coaxial with the axis of the ellipsoid of deformation (Bouchez et al., 1997). So, the magnetic lineation corresponds to K1 while K3 is the pole of the magnetic foliation.

The main scalar data provided by the AMS measurements are:

- Bulk susceptibility (Km) : Km = 1/3 (K1 + K2 + K3)

- Total anisotropy degree (P) : P = K1/K3

- The shape factor (T): T = [Log(K2/K3)-Log(K1/K3)]/[Log(K2/K3)+Log(K1/K2)]

The raw data have been computed using the Anisoft software of Agico which allow to calculate for each parameter the mean value of all the samples of the same sampling station and also allow to appreciate the more or less best grouping of directional data (lineations and foliations) via the statistics provides by the degree of confidence and the ellipse of confidence (see appendix).

For the microstructure studies, the thin sections have been performed and observed under optical microscope at the Laboratoire Géosciences et Environnement (LaGE) of Université Joseph KI-ZERBO.

In order to characterize the carriers of the ferromagnetic magnetization, the measurements of magnetic susceptibility versus temperature have been performed on a few numbers of samples having Km ≥ $500x10^{-6}$ SI units using the CS-3 apparatus coupled to the Kappabridge KLY-3.

Since the aeromagnetic data allow to access deep structures on non-outcroping areas, in this study, we used an image of already processed data by BUMIGEB (2015). This image obtained by processing total magnetic intensity (TMI) data with the OASIS MONTAJ software of GEOSOFT.

4. Results

4.1. Scalar data analysis

Up to now the proposed limits between magnetic susceptibilities dominated by the contributions of the paramagnetic particles and those dominated by the contributions of the ferromagnetic particles are based on empirical observations (Rochette, 1987; Bouchez, 1997; Trindade et al., 1999). When consider a magnetic susceptibility of $500x10^{-6}$ SI units as a limit

between paramagnetic and ferromagnetic behaviours (Bouchez, 1997), in our case, the ferromagnetic stations are dominant (Tables 1, 2, 3, 4 and Fig.4).

Measurements of magnetic susceptibility versus temperature have been performed in order to carry out the nature of the particles responsible of the ferromagnetic behaviour.

The experimental graphs show a complete loss of magnetic susceptibility at a temperature of 580°C (Fig. 5). This temperature corresponds to the Curie temperature of magnetite and/or titanomagnetite. When cooling the sample, the reconstitution of the magnetic susceptibility begins at the same temperature but not reach to the same values before the heating. This mean that the destabilized magnetite during the heating is not entirely reconstituted.

The range of the granitic plutons and their country rocks shape factor values are between -0.75 and 0.81 with a maximum of values between -0.5 and 0.5 (Tables 1, 2, 3, 4). The maximum of the values between -0.5 and 0.5 mean that the fabric is overall plano-linear with predominantly flattening ($0 < T \leq 0.81$). Planar fabric stations are 75 % of the stations in the Dori pluton, 60 % of the stations in the Gorom-Gorom pluton and 50 % of the stations in the Touka Bayèl pluton.

On the map views, the surfaces of all the plutons are almost entirely occupied by shape factors more than 0 (oblate ellipsoids). The shape factors less than 0 (prolate ellipsoids), less numerous, occurred as small surfaces randomly distribute (Fig. 6).

The total anisotropy degree varies from 1.02 to 1.44 for all the plutons. The values are less than 1.15 for 86.90 % of the sampling stations in the Dori pluton, 80.15 % of the sampling stations in the Gorom-Gorom pluton and 58.82 % of the sampling stations in the Touka Bayèl pluton. These values of the total anisotropy degree are low for magnetite-bearing granites. On the map views, the surfaces of all the plutons are almost entirely occupied by anisotropy degree less than 1.15. The total anisotropy degree more than 1.15, less numerous, are observed into small surfaces randomly distribute (Fig. 7).

The graphs of P versus T show that there is no correlation between two parameters (Fig.8).

4.2. Magnetic lineation

The magnetic lineation in the Dori pluton is approximately oriented E-W and slightly arcade in the Northern part of the pluton (Fig. 9a). The slightly to moderately plunging lineation (0° to 59°) represent 59 % of the stations, except in the southern half of the pluton where steeply

plunging lineations (≥ 60°) cover more important surface. The lower hemisphere equal-area projection diagram indicates that the mean line of the magnetic lineation within the pluton is 288°/82° (Fig. 9b).

In the Gorom-Gorom pluton, the slightly to moderately plunging magnetic lineation are more frequent (54 %). The steeply plunging magnetic lineation are observed in small clusters by location. The organization of the slightly to moderately plunging magnetic lineation is consistent by sector and allows to distinguish two sectors namely sectors A and B (Fig. 10a, b and c). On one hand, in the Sector A, the trends of the magnetic lineation are approximately oriented NE-SW with a mean line at 207°/75° (Fig. 10b). On the other hand, in the Sector B, the trends are roughly N-S with a mean line at 205°/57° (Fig. 10c).

For the Touka Bayèl pluton (Fig. 10a), the moderately plunging lineations represent 94 % of the magnetic lineations and the lower hemisphere equal-area projection diagram indicates a mean orientation of the magnetic lineation at 224°/43° (Fig. 10d).

The orientations of the slightly to moderately plunging magnetic lineations of the country rocks have an NNE-SSW average trend, especially near the Tiébélé-Dori-Markoye fault (Figs. 9 and 10) and secant on those of the granitic plutons.

4.3. Magnetic foliation

In biotite granite plutons and their country rocks, the magnetic foliation is steeply dipping (≥ 60°) for about 68 % of the stations.

The nearby country rock magnetic foliation is approximately parallel to the granitic pluton contact and the internal foliation of Dori pluton (Fig. 11a).

The internal pattern of the Dori pluton is concentric with a small core in the southeastern part and a slightly larger one in the southwestern part (Fig. 11a). The lower hemisphere equal-area projection diagram indicates that the mean pole of the magnetic foliation of the whole pluton is 167°/9° (Fig. 11b).

The magnetic foliations of the country rock around of the Gorom-Gorom pluton are secant on the western border while to the east, it is partly controlled by the Tiébélé-Dori-Markoye fault which is oriented NE-SW (Fig. 12a).

The organization of the internal magnetic foliations of this pluton is coherent into four sectors A, B_1, B_2 and B_3). In the sector A, the magnetic foliation trend is approximately E-W while in the three other sectors (B_1, B_2, and B_3), the patterns of the magnetic foliations are concentric similar to that observed in the Dori pluton (Fig. 12a). The lower hemisphere equal-area projection diagrams indicate that for the sectors A, B_1, B_2 and B_3, the means poles of the magnetic foliation are respectively 354°/14°, 24°/39°, 79°/16° and 103°/19° (Fig. 12b, c, d and e).

The magnetic foliations of the Touka Bayèl pluton have also concentric pattern with dominantly medium-dipping (Fig. 12a). The lower hemisphere equal-area projection diagram indicates a mean pole at 69°/49° (Fig. 12f)

4.4. Microstructures

In the biotite granites and their close country rocks, three types of microstructures are clearly distinguished : (i) magmatic microstructures in which the minerals are stable and unscathed from any deformation (Fig. 13a and b).This type of microstructure is well expressed and is largely predominant in biotite granites and their hosts rocks, (ii) high-temperature solid-state deformation microstructures which are essentially expressed by flexured plagioclases denoting that they were still softened at the moment of the deformation (Fig. 13c) and (iii) low-temperature deformation microstructures which are characterized by recrystallization of quartz crystals into sub-grains with poorly restored contours and highly marked rolling extinction (Fig. 13d). As expected, these last two microstructures are generally observed at the edge of the pluton or near the major shear zone.

The cartographic distribution of the microstructures in the three plutons and their close country rocks shows that the magmatic microstructures are abundant compared to the low temperature and high temperature deformation microstructures (Fig. 14a and b). Low-temperature deformation microstructures are observed in the country rocks along the major Tiébélé-Dori-Markoye shear zone. At the border of the Dori and Gorom-Gorom plutons, some microstructures express a continuum of deformation from high temperature to low temperature.

5. Discussion

The magnetic susceptibility values by station shows that ferromagnetic stations predominate both in biotite granites and in their TTG-country rocks. The carriers of the magnetization in this

297 case have been identified as magnetite and/or titano-magnetite (Vegas et al., 2008; Traore et
298 al., 2011; Salazar et al., 2013).

299 The total anisotropy degree (P = K1/K3) in general is correlated with the rate of deformation.
300 This is especially true for paramagnetic granitoids in which the contribution to the total
301 anisotropy degree is dominated by the iron-bearing silicates (Archanjo et al., 1995; Bouchez,
302 1997; Gleizes et al, 1998; Bella Nke et al., 2022). In the ferromagnetic granitoids, the total
303 anisotropy degree is mainly based on the shape fabric of the magnetite and evenly the
304 anisotropy related to interactions between the magnetite grains due to their distribution in the
305 rock (Gregoire et al., 1995; Gregoire et al., 1998). In this case, the total anisotropy degree
306 doesn't reflect absolutely the rate of deformation (Archanjo et al., 1992; Bouchez, 1997; Naba
307 et al., 2004; Sawadogo et al., 2018).

308 The values of the shape factor, between -0.75 and 0.81, are consistent with a plano-linear
309 fabric with a slight predominance of the flattening since $T > 0$ in most of the cases. This
310 suggests that both linear and planar fabrics are well expressed and indicates that flattening
311 deformation was dominant.

312 The emplacement mechanisms of plutons still a matter of debate up to now (Clemens and
313 Mawer, 1992; Karlstrom et al., 1993; Paterson and Fowler, 1993; Pons et al., 1995; Bouchez,
314 1997; Vegas et al., 2008; Nédélec and Bouchez, 2011; Njiki Chatué et al., 2020). In all cases
315 the raw data that allow this kind of discussion are whole shapes of the plutonic intrusions
316 (rounded or elongate) and especially their internal fabrics (foliations and lineations). Thus, the
317 overall concentric fabrics centered on the pluton's core, parallel to it limits and to the fabrics of
318 the country rocks might correspond to a diapiric body (Ramsay, 1989; Pons et al., 1995; Vegas
319 et al., 2008). When the plutonic body is a result from magma ascent through fractures and their
320 accumulation into a dilatational structures (Scaillet et al., 1995; Petford, 1996), the trends of
321 the fabrics don't vary a lot over the surface of the whole pluton. Also, the fabrics of the pluton
322 are not necessarily parallel to those of country rocks.

323 In all cases the rheology of country rocks at the moment of the emplacement determines the
324 intrusion shape and the dispositions of it internal structures (Choukroune, 1995).

When regional stresses are actives at the moment of the emplacement, they may also control partially the shape and the orientations of the internal fabrics (Bouchez, 1997; Nédélec and Bouchez, 2011 and references therein).

For the present study, the directional data allowed to highlight the internal fabric of the plutons. Indeed, in the Dori pluton as well as in sectors B_1, B_2 and B_3 of the Gorom-Gorom pluton and the Touka Bayèl pluton, the concentric patterns of foliation trajectories are compatible with inflation during magma ascent (Gleizes et al., 2006) and express a diapiric emplacement of these plutons (Vegas et al., 2008; Njiki Chatué et al., 2020; Bella Nke et al., 2022). Sector A of the Gorom-Gorom pluton is a large E-W oriented dyke (Scaillet et al., 1995; Petford, 1996). Furthermore, the organization of the granitic pluton fabrics suggests that the large Gorom-Gorom pluton is made up of small coalescent plutons whereas the Dori and Touka Bayèl plutons are homogeneous bodies.

The slightly to moderately plunging magnetic lineations associated with steeply dipping magnetic foliations reflect an interference between magmatic ascent and the regional stresses. These lineations express therefore the finite stretch at least during the final increments of magmatic strain (Bouchez, 1997). This observation is testified by the microstructures still magmatic on many sampling stations. The steeply plunging lineations, which occupy more or less well individualized clusters in the plutons, are interpreted as magma feeding zones (Vigneresse and Bouchez, 1997; Naba et al., 2004; Vegas et al., 2008). For some stations on the borders of the plutons, the fabric is clearly controlled by the regional deformation along the shear zones since the microstructures there, are of solid state.

Except the parts reworked by the plutons inflation or overprint by the shear zones, the foliations in the host rocks have NE-SW orientation.

The emplacement mechanisms evidenced on one hand through the magnetic foliation trajectories and the trends and plunges of the lineations and other hand, from microstructures studies show that some of the plutons were emplaced in a fairly softened crust while in the same period the northern part of the Gorom-Gorom pluton was subject of a big tension gash at a relatively high level in an already cooled crust. Such a contrasting rheological context for the same geological environment, is a similar case that was argued by Pons et al. (1995) in western Niger and Vegas et al. (2008) in eastern Burkina Faso.

The radiometric ages of Dori pluton (2164 Ma) and Gorom-Gorom pluton (2148 Ma) and those of the TTG host rocks, around 2210 to 2100 Ma (Castaing et al., 2003; Tshibubudze et al., 2015), can indicate that the time span of emplacement of the granitic plutons overlap that of the TTGs of the Dori area and so, may justify the still softening behaviour of the crust during the emplacement of biotite granite plutons.

In accordance with the range of the ages of the emplacement of the TTGs of whole Baoulé-Mossi domain (Parra-Avila et al., 2016; Parra-Avila et al., 2019; Masurel et al., 2021), we can consider that the granitoids of Dori area correspond to one of the older terranes since the latter granitoids (biotite granites here studied) of this area are older than the TTGs of the other areas.

The ages and the orientations of the D1 event of Eburnean orogeny vary from one locality to another (see synthesis in Grenholm, et al., 2019). The D1 event identified in the study area (Tshibubudze et al., 2013; Hein, 2010) is NE oriented and is supposed to last between 2130 and 2105 Ma. So, the emplacement of the Dori and Gorom-Gorom plutons which precede this D1, also called Tangaean event might correspond to the $D_{1\text{-}x}$ or Pre-Tangaean phase of Hein, 2010.

In the present study, we clearly demonstrated through the orientations of fabrics from AMS measurements that the stresses during this D1-x or Pre-Tangaean event are E-W oriented and are later accommodated in a continuum of deformation by regional shear zones (e.g : some branches of the Tiébélé-Dori-Markoye shear zone).

The young Birimian crust was thin enough to undergo both rapid cooling and warming which allow the coexistence of vertical transfer of magmatic masses and transcurrent tectonics (Vegas et al., 2008). The following emplacement models (Fig. 14) can therefore be proposed for the Dori, Gorom-Gorom and Touka Bayèl plutons.

At the bottom of each block diagram, we can see the vertical ascent of the magma indicated by the red arrows. On the top of the block diagrams, we notice that the overall orientation of the fabrics are concentric for the sectors B_1, B_2, B_3 of the Gorom-Gorom pluton (Fig.14a), the Touka Bayèl pluton (Fig.14b) and Dori pluton (Fig.14c), reflecting an emplacement in a softened crust. The regular fabrics following an E-W trend in the northern part of the Gorom-Gorom pluton might reflect a fracture-like site of collection of the magma following the maximum stress orientation at the moment of the emplacement.

After this stage and into a continuum of deformation, the regional shear zones affects some boundaries of the already emplaced plutons.

6. Conclusion

Through this study, we have shown that between 2200 Ma and 2100 Ma the rheology of the crust, in Dori area (Northeastern Burkina Faso), was quite contrasted, authorizing an emplacement of the magma according to two different mechanisms for the same environment: (i) diapirism for the Dori pluton, the Touka Bayèl pluton and the sectors B_1, B_2 and B_3 of the Gorom-Gorom pluton and (ii) along a big tension gash for the sector A of the Gorom-Gorom pluton.

The emplacement of these granitic plutons in Dori area probably correspond to an early episode of the Eburnean orogeny. The regional tectonics of this period corresponds to an E-W shortening which was later accommodated by a regional transcurrent NE-SW dextral shearing. This study allows to understand the rheological context of the emplacement of the studied granitic plutons and brings new arguments on the tectonic style at this early period of the Eburnean orogeny.

ACKNOWLEDGMENTS: This work was carried out with the financial support of the WAXI2 Program and the logistical support of the Institut de Recherche pour le Développement (IRD).

References

- Ama Salah I., Liegeois J.P., Pouclet A. 1996. Evolution d'un arc insulaire océanique birimien précoce au Liptako Nigérien (Siriba): géologie, géochronologie et géochimie. Journal of African Earth Sciences 22, 235–254.

Abouchami W., Boher M., Michard A., Albarède F., 1990. A major 2.1 Ga old event of mafic magmatism in West Africa: an early stage of crustal accretion. J. Geophys. Res., 95 (B11), 17, 605-629

- Amponsah-Tawiah K., Mensah J. (2016). Occupational Health and Safety and Organizational Commitment: Evidence from the Ghanaian Mining Industry. Safety and Health at Work, 7(3), 225–230. doi:10.1016/j.shaw.2016.01.002

412 - Archanjo C. J., Olivier P., Bouchez J.-L. 1992. Plutons granitiques du Serido (NE du Brésil) :
413 écoulement magmatique parallèle à la chaine révélée par leur anisotropie magnétique Bull. Soc.
414 Géol. France, t. 163, n°4, pp. 509-520

415 - Archanjo C. J., Launeau P. et Bouchez J. L., 1995. Magnetic fabric vs. Magnetite and biotite
416 shape fabrics of the magnetite-bearing granite pluton of Gameleiras (Northeast Brazil). Phys.
417 earth plan. Inter. 89: 6375.

418 - Baratoux L., Metelka V., Naba S., Jessell M.W., Gregoire M., Ganne J., 2011. Juvenile
419 Paleoproterozoic crust evolution during the Eburnean orogeny (~2.2–2.0 Ga), western Burkina
420 Faso. Precambrian Research 191, 18–45.

421 - Baratoux L., Metelka V., Naba S., Ouiya P., Siebenaller L., Jessell M.W., Naré A., Salvi S.,
422 Béziat D., Franceschi G. 2015. Tectonic evolution of the Gaoua region, Burkina Faso:
423 Implications for Mineralization. Journal of African Earth Sciences 112, 419-439

424 - Baratoux L., Söderlund U., Ernst R. E., de Roever E., Jessell M. W., Kamo S., Naba S.,
425 Perrouty S., Metelka V., Yatte D., Grenholm M., Diallo D. P., Ndiaye P. M., Dioh E., Cournède
426 C., Benoit, M., Baratoux D., Youbi N., Rousse S. and Bendaoud, A. 2019. New U–Pb
427 Baddeleyite Ages of Mafic Dyke Swarms of the West African and Amazonian Cratons:
428 Implication for Their Configuration in Supercontinents Through Time. Springer Geology,
429 https://doi.org/10.1007/978-981-13-1666-1_7

430 - Belle Nke B. E., Njanko T., Mamtani M. A., Rochette P., Njonfang E. 2022. Time relationship
431 between emplacement, fabric development and regional deformation of the Manchi granitic
432 pluton (western - Cameroon domain)-an integrated AMS, CPO and microstructural
433 investigation. Journal of Structural Geology 160(2–3):104619

434 - Beziat D., Bourges F., Debat P., Lompo M., Martin F., Tollon F. 2000. A Paleoproterozoic
435 ultramafic–mafic assemblage and associated volcanic rocks of the Boromo greenstone belt:
436 fractionates originating from island-arc volcanic activity in the West African craton.
437 Precambrian Research 101, 25–47.

438 - Block S., Baratoux L., Zeh A., Laurent O., Bruguier O., Jessell M. W., Ailleres L., Sagna R.,
439 Parra-Avila L. A., Bosch D. 2016. Paleoproterozoic juvenile crust formation and stabilisation

in the south-eastern West African Craton (Ghana); New insights from U-Pb-Hf zircon data and geochemistry. Precambrian Research 287, 1–30

- Bouchez J. L., 1997. Granite is never isotropic: an introduction to AMS studies of granitic rocks. In J.L. Bouchez, D.H.W. Hutton and W.E. stephens (eds.), Granite: from segregation of melt to emplacement fabrics, Kluwer Acad. Publ., Dordrecht, 1997, 95-112.

- Boher M., Abouchami W., Michard A., Albarède F., Arndt T N., 1992. Crustal growth in West Africa at 2.1 Ga. J. Geophys. Res. 97, 345-369

- BUMIGEB, 2015. Levé géophysique aéroporté haute résolution en magnétisme et spectrométrie gamma du quart Nord-Est du Burkina Faso. Projet PADSEM (Programme d'Appui au Développement du Secteur Minier). Ministère des Mines et des Carrières.

- Castaing C., Billa M., Milési J.P., Thiéblemont D., Le Métour J., Egal E., Donzeau M. (BRGM) (coordonnateurs), Guerrot C., Cocherie A., Chèvremont P., Tegyey M., Itard Y. (BRGM), Zida B., Ouédraogo I., Koté S., Kaboré B.E., Ouédraogo C. (BUMIGEB), Ki J.C., Zunino C. (ANTEA), 2003. Notice explicative de la carte géologique et minière du Burkina Faso à 1/1 000 000. Edit. B.R.G.M., Orléans, France, p.147.

- Clemens J. D. and Mawer C. K. 1992. Granitic magma transport by fracture propagation. Tectonophysics, 204: 339-360.

- Chardon D., Bamba O., Traoré K. 2020. Eburnean deformation pattern of Burkina Faso and the tectonic significance of shear zones in the West African craton. BSGF-Earth Sciences Bulletin 2020, 191, 2

- Choukroune P. 1995. Déformation et déplacements dans la croûte terrestre. Edit. Masson, 224 p.

- Dampare S.B., Shibata T., Asiedu D.K., Osae S., Banoeng-Yakubo B. 2008. Geochemistry of Paleoproterozoic metavolcanic rocks from the southern Ashanti volcanic belt, Ghana: Petrogenetic and tectonic setting implications

- Doumbia S., Pouclet A., Kouamelan A., Peucat J.J., Vidal M, Delor, C., 1998-Petrogenesis of juvenile-type Birimian (Paleoproterozoic) granitoids in central Côte-d'Ivoire, West Africa: geochemistry and geochronology. Precambrian Research 87 (1–2): 33–63.

- Egal E., Thiéblemont D., Lahondère D., Guerrot C., Costea C. A., Iliescu D., Delor C., Goujou J.-C., Lafon J. M., Tegyey M., Diaby S., Kolié P. 2002. Late Eburnean granitization and tectonics along the western and northwestern margin of the Archean Kénéma–Man domain (Guinea, West African Craton). Precambrian Research 117, 57–84

- Eglinger A., Thébaud N., Zeh A., Davis J., Miller J., Parra-Avila L. A., Loucks R., McCuaig C., Belousova E. 2017. New insights into the crustal growth of the Paleoproterozoic margin of the 185 Archean Kéména-Man domain, West African craton (Guinea): Implications for gold mineral system. Precambrian Research 292, 258–289

- Feybesse J. L., Milési, J. P. (1994). The Archaean/Proterozoic contact zone in West Africa: a mountain belt of décollement thrusting and folding on a continental margin related to 2.1 Ga convergence of Archaean cratons? Precambrian Research, 69(1-4), 199–227. doi:10.1016/0301-9268(94)90087-6

- Feybesse J.L., Billa M., Guerrot C., Duguey E., Lescuyer J.L., Milesi J.P., Bouchot V. 2006. The Paleoproterozoic Ghanaian province : geodynamic model and ore controls, including regional stress modeling. Precambrian Research 149, 149– 196.

- Ganne J., De Andrade V., Weinberg R.F., Vidal O., Dubacq B., Kagambega N., Naba, S., Baratoux L., Jessell M., Allibon J. 2011. Modern-style plate subduction preserved in the Paleoproterozoic West African Craton. Nature Geoscience5

- Gasquet D., Barbey P., Adou M., Paquette J.L. 2003. Structure, Sr–Nd isotope geochemistry and zircon U–Pb geochronology of the granitoids of the Dabakala area Côte d'Ivoire: evidence for a 2.3 Ga crustal growth event in the Palaeoproterozoic of West Africa. Precamb. Res. 127, 329–354.

- Gleizes G., Crevon G., Asrat A., Barbey P. 2006. Structure, age and mode of emplacement 671 of the Hercynian Bordères-Louron pluton (Central Pyrenees, France). International 672 Journal of Earth Sciences, 95 (6), 1039-1052.

- Gleizes G., 1992 - Structure des granites Hercyniens des Pyrénées de Mont-Louis-Andorre à la Maladeta. Thèse Univ. Toulouse III, France, 259 p.

- Gleizes G., Leblanc D., Santana V., Olivier P., Bouchez J.L., 1998. Sigmoidal structures featuring dextral shear during emplacement of the Hercynian granite complex of Cauterets Panticosa (Pyrenees). J. Struct. Geol., 20 (9-10), 1229-1245

Grégoire V., de Saint-Blanquat M., Nédélec A., Bouchez J.L. (1995) Shape anisotropy versus magnetic interactions of magnetite grains: experiments and application to AMS in granitic rocks, Geophys. Res. Letters 22, 2765-2768.

- Grégoire V., Darrozes J., Gaillot P., Nédélec A., Launeau, P. 1998. Magnetite grain shape fabric and distribution anisotropy vs rock magnetic fabric: a three-dimensional case study. J. Struct. Geol., 20 (7), 937-944

- Grenholm M., Jessell M., Thébaud N. 2019. A geodynamic model for the Paleoproterozoic (ca. 2.27–1.96 Ga) Birimian Orogen of the southern West African Craton – Insights into an evolving accretionary-collisional orogenic system. *Earth-Science Reviews 192*. 138-193

- Hein K. A. A., 2010. Succession of structural events in the Goren Greenstone belt (Burkina Faso): implications for West African tectonics. Journal of African Earth Sciences 56, 83–94.

- Hirdes W., Davis D.W., Lüdtke G., Konan G., 1996. Two generations of Birimian Paleoproterozoic volcanic belts in northeastern Côte d´Ivoire West Africa: consequences for the Birimian controversy. Precamb. Res. 80, 173-191.

- Karlstrom K. E., Miller C. F., Kingsbury J. A. and Wooden J. L. 1993. Pluton emplacement along an active ductile thrust zone Piute Mountains, Southeastern California: Interaction between deformation and solidification processes. Geol. Soc. Am. Bull., 105: 213-230.

- Liégeois J.P., Claessens W., Camara D., Klerkx J. 1991. Short-lived Eburnian orogeny in southern Mali. Geology, tectonics, U-Pb and Rb-Sr geochronology. Precambr. Res. 50 (1–2), 111–136.

- Lompo M., Bourges F., Debat P., Lespinasse P., Bouchez J. L., 1995. Mise en place d'un pluton granitique dans la croûte birimienne fragile : fabrique magnétique du massif de Tenkodogo (Burkina Faso). C. R. Acad. Sci Paris, 320, série Il a, p. 1211-1218.

- Lompo M. (2009). Geodynamic evolution of the 2.25-2.0 Ga Palaeoproterozoic magmatic rocks in the Man-Leo Shield of the West African Craton. A model of subsidence of an oceanic

plateau. Geological Society, London, Special Publications, 323(1), 231–254. doi:10.1144/sp323.11

- Lompo M., 2010. Paleoproterozoic structural evolution of the Man-Leo Shield (West Africa). Key structures for vertical to transcurrent tectonics. Journal of African Earth Sciences 58, 19–36

- Masurel Q., Eglinger A., Thébaud N., Allibone A., André-Mayer A.-S., McFarlaneH., Miller J., Jessell M., Aillères L., Vanderhaeghe O., Salvi S., Baratoux L., Perrouty S., Begg G., Fougerouse D., Hayman P., Wane O., Tshibubudze A., Parra-Avila L., Kouamélan A., Amponsah P. O., 2021. Paleoproterozoic gold events in the southern West African Craton: review and synopsis. Mineralium Deposita. doi.org/10.1007/s00126-021-01052-5

- McCuaig T.C., Fougerouse D., Salvi S., Siebenaller L., Parra-Avila L. A., Seed R., Béziat D., André-Mayer A.-S., 2016. The Inata deposit, Belahouro District, northern Burkina Faso. Ore Geology Review 78, 639-644.

- Mériaud N., Thébaud N., Masurel Q., Hayman P., Jessell M., Kemp A., Evans N.J., Fisher C.M., Scott P.M., 2020. Lithostratigraphic evolution of the Bandamian Volcanic Cycle in central Côte d'Ivoire: Insights into the late Eburnean magmatic resurgence and its geodynamic implications. Precambrian Res. 347, 105847.

- Milési J.P., Feybesse J.L., Ledru P., Dommanget A., Ouédraogo M.F., Marcoux E., Prost A., Vinchon C., Sylvain J.P., Johan V., Tegyey M., Calvez J.Y. et Lagny P. 1989. Les mineralisations auriferes de l'Afrique de I'Quest : Leurs relations avec I'evolution lithostructurale au Proterozoique inferieur. Chron. rech. min., n" 497, pp. 3-98.

- Milési J.P., Ledru P., Ankrah P., Johan V., Marcoux E., Vinchon Ch., 1991. The metallogenic relationship between Birimian and Tarkwaian gold deposits in Ghana. Mineralium Deposita 26, 228–238.

- Naba S., Lompo M., Debat P., Bouchez J.L., Beziat D., 2004. Structure and emplacement model for late-orogenic Palaeoproterozoic granitoids: the Tenkodogo-Yamba elongate pluton (Eastern Burkina Faso). J. Afr. Earth Sci. 38, 41–57.

- Njiki Chatué C., Njanko T., Fozing E.M., Bella Nké B.E., Séta N., Njonfang E., 2020. Field observations, magnetic fabrics and microstructures evidences of syn-kinematic emplacement of the Numba granitic pluton (western Cameroon domain). J. Afr. Earth Sci. vol. 172

- Ouiya P., Siebenaller L., Salvi S., Béziat D., Naba S., Baratoux L., Franceschi, G. (2016). The Nassara gold prospect, Gaoua District, southwestern Burkina Faso. Ore Geology Reviews, 78, 623–630. doi:10.1016/j.oregeorev.2015.11.026

- Parra-Avila L.A., Belousova E., Fiorentini M.L., Baratoux L., Davis J., Miller J., McCuaig T.C., 2016. Crustal evolution of the Paleoproterozoic Birimian terranes of the Baoulé-Mossi domain, southern West African Craton: U-Pb and Hf-isotope studies of detrital zircons. Precambr. Res. 274, 25–60.

- Parra-Avila L. A., Baratoux L., Eglinger A., Fiorentini M. L., Block S.. 2019. The Eburnean magmatic evolution across the Baoulé-Mossi domain: Geodynamic implications for the West African Craton. Precambrian Research 332, 105392

- Paterson S. R. and Fowler T. K. 1993. Re-examining pluton emplacement processes. J. Struct. Geol., 15 (2): 191-206.

- Pawlig S., Gueye M., Klischies R., Schwarz S., Wemmer K., Siegesmund S., 2006. Geochemical and Sr–Nd isotopic data on the Birimian of the Kedougou-Kenieba Inlier (Eastern Senegal): implications on the Paleoproterozoic evolution of the West African Craton. South African Journal of Geology 109, 411–427.

- Perrouty S., Aillères L., Jessell M., Baratoux L., Bourassa Y. 2012. Revised Eburnean geodynamic evolution of the gold-rich southern Ashanti Belt, Ghana, with newfield and geophysical evidence of pre-Tarkwaian deformation. Precambr. Res.204, 12–39.

- Petersson A., Scherstén A., Kempb A.I.S., Kristinsdóttira B., Kalvigc P., Anum S. 2016. Zircon U–Pb–Hf evidence for subduction related crustal growth andreworking of Archaean crust within the Palaeoproterozoic Birimian terrane, West African Craton, SE Ghana. Precambrian Research 275, 286–309

- Petford N., 1996. Dykes or diapirs ? Trans. Roy. Soc. Edinburgh: Earth Sci. 87, 105-114.

- Pons J., Oudin C., Valero J., 1992 - Kinematics of large syn-orogenic intrusions example of the Lower Proterozoic Saraya batholith (Eastern Sénégal). Geologische Rundschau, 81/2, 473-486, Stuttgart

- Pons J., Barbey P., Dupuis D., Léger J.M. 1995. Mechanisms of pluton emplacement and structural evolution of a 2.1 Ga juvenile continental crust : the Birimian of southwestern Niger. Precamb. Res. 70, 281-301.

- Pouclet A., Vidal M., Delor C. Siméon Y. et Alric G. 1996. Le volcanisme birimien du nord-est de la Côte-d'Ivoire, mise en évidence de deux phases volcano-tectoniques distinctes dans l'évolution géodynamique du Paléoprotérozoïque. Bull. Soc. géol, France, 1996, t. 167, nO 4, pp. 529-541

- Ramsay. 1989. Emplacement kinematics of a granite diapir: the Chindamora batholith, Zimbabwe, J. Struct. Geol. 11: 191-209.

- Salazar C. A., Archanjo Carlos J., Rodrigues S. W. de O., Hollanda M. H. B. M., Liu D., 2013. Age and magnetic fabric of the Três Córregos granite batholith: evidence for Ediacaran transtension in the Ribeira Belt (SE Brazil). Int J Earth Sci (Geol Rundsch), 102, 1563–1581

- Sawadogo S., Naba S., Ilboudo H., Traoré A. S., Nakolendoussé S., Lompo M. 2018. The Belahourou granite pluton (Djibo greenstone belt, Burkina Faso) : emplacement mechanism and implication for gold mineralization along a shear zone. Journal of African Earth Sciences, 148, 59-68

- Scaillet B., Pêcher A., Rochette P. and Champenois, M. 1995. The Gangotri granite (Garhwal Himalaya): Laccolithic emplacement in an extending collisional belt. J. Geophys. Res. 100, B1, p. 585-607.

- Soumaila A., Henry P., Rossy M. (2004). Contexte de mise en place des roches basiques de la ceinture de roches vertes birimienne de Diagorou-Darbani (Liptako, Niger, Afrique de l'Ouest) : plateau océanique ou environnement d'arc/bassin arrière-arc océanique. Comptes Rendus Geoscience, 336(13), 1137–1147. doi:10.1016/j.crte.2004.03.008

- Soumaila, A et Garba Z, 2006. Le métamorphisme des formations de la ceinture de roches vertes Birimiennes (Paléoprotérozoïque) de Diagorou-Darbani (Liptako,Niger, Afrique de l'ouest). Africa Géosciences Review, Vol. 3, N°1, 107-128

606 - Sylvester P. J., & Attoh K. (1992). Lithostratigraphy and Composition of 2.1 Ga Greenstone
607 Belts of the West African Craton and Their Bearing on Crustal Evolution and the Archean-
608 Proterozoic Boundary. The Journal of Geology, 100(4), 377–393. doi:10.1086/629593

609 - Tapsoba B., Lo C.-H., Jahna B.-M., Chunga S.-L., Wenmenga U., IizukaY. 2013.Chemical
610 and Sr–Nd isotopic compositions and zircon U–Pb ages of the Birimian granitoids from NE
611 Burkina Faso, West African Craton: Implications on the geodynamic setting and crustal
612 evolution

613 - Taylor N.P., Moorbath S., Leube A., Hirdes W., 1992. Early Proterozoic crustal evolution in
614 the Birimian of Ghana: constraints from geochronology and isotope geochemistry. Precambrian
615 Res. 56, 97–111

616 - Traoré A. S., Naba S., Kagambéga N., Lompo M., Baratoux L., Ganne J.. 2011. Mise en place
617 tardi-orogenique de la syénite de Wayen (Burkina Faso, Afrique de l'Ouest). J. Sci.Vol. 11, N°
618 2, 1 – 15

619 - Traore K., Chardon D., Naba S., Wane O., Bouare M.L. 2022. Paleoproterozoic collision
620 tectonics in West Africa: Insights into the geodynamics of continental growth *Precambrian*
621 *Research* 376

622 - Tshibubudze A. et Hein, K. A. A. 2013. Structural setting of gold deposits in the Oudalan-
623 Gorouol volcanosedimentary belt east of the Markoye Shear Zone, West African Craton Journal
624 of African Earth Sciences 80, 31–47

625 - Tshibubudze A., Hein K. A. A., McCuaig T. C. 2015. The relative and absolute chronology
626 of strato-tectonic events in the Gorom-Gorom granitoidterrane and Oudalan-Gorouol belt,
627 northeast Burkina Faso. Journal of African Earth Sciences 112, 382-418

628 - Tshibubudze A., Hein K. A. A., 2016. Gold mineralisation in, the Essakane goldfield in
629 Burkina Faso, West African craton. Ore Geology Reviews. Journal of African Earth Sciences
630 112 (2015) 382-418.

631 - Vegas N., Naba S., Bouchez J.L., Jessell M. W. 2008. Structure and emplacement of granite
632 plutons in the Paleoproterozoic crust of Eastern Burkina Faso: rheological implications. Intern.
633 J. Earth Sci., 97, 1165–1180.

- Vidal M., Delor C., Pouclet A., Simeon, Y., Alric G., 1996. Evolution géodynamique de l'Afrique de l'Ouest entre 2.2 Ga et 2 Ga: le style archéen des ceintures vertes et des ensembles sédimentaires Birimiens du Nord-Est de la Côte D'Ivoire. Bulletin de la société géologique de France 167, 307–319.

- Vidal M., Gumiaux C., Cagnard F., Pouclet, A., Ouattara, G., Pichon, M., 2009. Evolution of a Paleoproterozoic "weak type" orogeny in the West African Craton (Ivory Coast). Tectonophysics 477, 145–159.

- Vigneresse J.L., Bouchez J.L., 1997. Successive granitic magma batches during pluton emplacement: the case of Cabeza de Araya Spain. J. Petrol. 38, 1767-1776.

- Wane O., Liégeois J-P, Thébaud N., Miller J., Metelka V., Jessell M. W. 2018. The onset of the Eburnean collision with the Kenema-Man craton evidenced by plutonic and volcanosedimentary rock record of the Masssigui region, southern Mali. Precambrian Research 305, 444–478

- Woodman K. K., Baratoux L., Somda A., Siebenaller L. 2016. The Youga gold deposit, Burkina Faso. Ore Geology Reviews, 78, 631–638. doi:10.1016/j.oregeorev.2015.11.0

- Yaméogo A. O., Naba, S., Traoré, S. A. 2020. Caractères pétrographiques et Géochimiques des granitoïdes de la région de Dori au Nord-Est du Burkina Faso, Craton Ouest Africain. Afrique SCIENCE 16 (1), 375 – 395

Tables' captions

Table 1: Location of stations and magnetic data of the TTG-type host rock

Table 2: Location of stations and magnetic data of the Dori granitic pluton

Table 3: Location of stations and magnetic data of the Gorom-Gorom granitic pluton

Table 4: Location of stations and magnetic data of the Touka Bayèl granite

Table 1

Stations	Coordinates	Scalar data			Directional data		Specimens numbers
	Long./Lat.	Km ($x10^{-6}$)	P	T	K1	K3	
DO006	-0.07549/13.87887	52892.20	1.45	-0.23	69/11	256/56	5
DO007	-0.07188/13.84254	57704.04	1.64	0.20	322/19	320/83	5
DO065	0.11759/14.01187	374.87	1.08	-0.31	263/42	100/72	6
DO067	0.14420/14.09254	264.28	1.08	0.81	0/59	196/81	6
DO068	0.16073/14.08051	355.42	1.07	-0.01	276/74	168/85	6
DO069	0.17403/14.07472	235.22	1.04	0.29	290/73	202/73	6
DO070	0.15404/14.06570	312.61	1.09	0.59	259/64	189/65	6
DO089	0.11936/14.03902	663.29	1.07	0.18	240/54	168/55	6
DO093	0.16641/13.99579	320.27	1.12	0.68	241/61	185/66	4
DO097	0.15056/14.10686	260.32	1.07	0.30	184/46	176/82	5
DO098	0.16235/14.10786	286.42	1.06	0.34	296/66	160/73	6
DO099	0.14942/14.12179	282.42	1.06	0.42	151/63	143/86	5
DO100	0.12888/14.12143	1177.57	1.06	0.52	176/59	148/75	6
DO110	0.02993/14.18669	3388.18	1.22	0.22	81/3	261/86	5
DO112	0.04806/14.20569	205.73	1.09	-0.02	120/54	113/85	4
DO116	-0.07181/14.22317	5513.33	1.04	-0.12	135/52	80/57	5
DO117	-0.31781/14.02084	1383.22	1.22	-0.41	257/58	211/66	5
DO118	-0.41852/14.01905	361.28	1.02	-0.07	186/40	185/89	5
DO119	-0.43690/14.01911	125.59	1.19	0.05	258/72	186/74	4
DO122	-0.54027/14.05817	372.05	1.07	-0.08	248/31	139/35	4
DO132	-0.06403/14.23791	5427.23	1.05	0.51	256/52	6/87	6
DO135	-0.12507/14.33632	16513.47	1.70	-0.31	265/49	237/69	4
DO142	-0.22064/14.12579	121081.47	1.20	0.68	296/67	296/90	5
DO152	-0.54352/14.08021	32930.31	1.17	-0.65	250/14	101/26	5
DO156	0.12472/13.85446	3004.83	1.07	0.44	31/65	264/70	5
DO157	0.07521/13.84762	198.28	1.07	-0.41	229/9	50/86	5
DO158	0.05960/13.83313	96.16	1.16	0.50	79/39	2/41	4
DO166	-0.03989/13.83877	442.36	1.05	0.10	357/63	331/78	6
DO167	-0.05852/13.85909	16712.14	1.38	0.05	257/22	256/82	8
DO168	-0.06008/13.84831	15731.76	1.52	-0.13	296/53	262/67	6
DO170	0.02032/13.83104	392.66	1.08	-0.34	349/70	222/74	5
DO179	-0.05970/13.87679	28247.03	1.54	0.13	304/38	125/89	6
DO183	0.14507/13.87194	2692.85	1.08	-0.12	280/53	232/61	6
DO184	0.16288/13.88650	202.67	1.12	0.19	28/69	354/77	6
DO186	0.11196/13.89601	1685.29	1.11	0.20	307/52	221/52	5
DO187	0.11631/13.90680	528.75	1.04	0.17	276/48	254/71	6
DO188	0.12912/13.91068	1958.51	1.19	0.46	270/42	246/66	6
DO191	0.18050/13.90969	68.92	1.13	0.04	357/0	357/13	5
DO192	0.18339/13.92703	174.91	1.08	0.11	179/3	0/74	5
DO193	0.16993/13.92600	100.98	1.21	0.49	20/25	356/48	8
DO195	0.12547/13.92830	455.21	1.09	0.49	242/50	212/67	6
DO200	0.14246/13.94733	993.77	1.30	0.68	259/68	189/69	5
DO202	0.18024/13.94565	205.11	1.08	0.76	111/25	24/29	4
DO204	0.13969/13.95283	409.40	1.16	0.59	267/60	201/62	6
DO205	0.12137/14.01434	44.24	1.14	-0.19	293/45	217/46	6
DO220	0.11238/14.11981	174.61	1.09	0.75	150/72	342/86	6

DO144	-0.33016/14.01690	69.33	1.07	0.01	249/61	198/68	4
DO146	-0.51399/14.03944	3150.55	1.22	-0.64	245/48	180/53	4
DO229	-0.03286/14.15918	316.01	1.08	0.25	170/54	357/85	5
DO231	0.05722/14.18897	349.45	1.07	0.09	96/63	301/77	6
DO232	0.09204/14.15946	278.76	1.10	0.53	145/83	349/87	5
DO233	-0.11115/13.84429	24421.69	1.24	-0.22	296/30	291/80	5
DO234	-0.09352/13.84343	24644.54	1.42	0.16	300/24	292/74	5
DO235	-0.11487/13.86052	20970.64	1.28	0.14	145/41	327/87	6
DO239	-0.08071/14.11044	212.16	1.03	-0.31	60/48	256/76	6
DO243	-0.09392/14.08271	287.85	1.07	-0.29	15/31	205/75	5
DO245	-0.11182/14.08469	281.59	1.05	0.06	88/56	49/67	6
DO253'	-0.13260/13.96979	656.34	1.08	0.20	73/55	45/72	7
DO265	-0.19687/13.93478	1443.11	1.06	0.17	260/13	255/32	4
DO266	-0.14770/13.91120	65237.15	1.94	-0.28	85/70	343/70	5
DO267	-0.15204/13.89663	40591.13	1.90	0.11	57/75	248/87	5
DO268	-0.13544/13.91355	58443.73	1.83	-0.25	269/76	224/72	6
DO272	-0.09513/13.90040	25110.23	1.73	0.19	62/83	306/84	4
DO273	-0.11191/13.91201	54625.06	1.89	-0.10	68/73	282/80	5
DO307	-0.18049/14.46131	9167.26	1.25	-0.09	102/13	99/83	4
DO311	-0.32212/14.40571	12104.60	1.20	-0.40	44/69	333/70	4
DO312	-0.35472/14.39860	66.33	1.02	-0.20	197/1	17/85	5
DO326	-0.19400/14.46296	9355.03	1.32	-0.08	88/1	87/47	5
DO327	-0.21794/14.45411	6701.94	1.41	0.06	275/11	105/47	6
DO328	-0.28920/14.44557	5549.59	1.19	0.70	249/22	99/40	5
DO330	-0.40269/14.43764	20776.25	1.13	-0.07	20/58	0/78	5
DO331	-0.41699/14.44286	14080.23	1.09	0.02	66/72	12/75	5
DO339	-0.49143/14.31109	4247.33	1.39	-0.10	199/64	172/77	4
DO221	0.11312/14.14534	293.59	1.07	0.19	105/59	315/73	5
DO222	0.09692/14.15240	258.71	1.05	-0.43	59/77	5/79	6
DO373	-0.16241/14.34357	3225.00	1.16	0.10	273/59	170/61	4
DO376	-0.18105/14.31142	8798.84	1.18	-0.11	264/64	153/65	6
DO377	-0.17389/14.30283	783.03	1.19	0.30	289/67	152/74	6
DO378	-0.16193/14.30952	1523.17	1.18	0.30	254/66	145/67	6
DO379	-0.16894/14.32453	4419.30	1.17	-0.13	256/63	242/83	6
DO380	-0.12740/14.29711	1584.15	1.25	-0.45	198/70	48/80	6
DO381	-0.14384/14.28967	6844.73	1.20	0.21	295/80	186/80	5
DO382	-0.14377/14.31310	5627.29	1.24	-0.65	230/54	86/67	5
DO383	-0.12507/14.31164	162.53	1.25	-0.63	277/75	189/75	4
DO384	-0.14377/14.32436	21105.70	1.41	0.40	286/75	123/85	6
DO387	-0.11699/14.34472	17026.79	1.41	-0.07	262/51	171/51	5
DO388	-0.47862/14.27892	1026.39	1.23	0.20	249/2	247/40	6
DO389	-0.46016/14.24986	6332.92	1.17	-0.06	264/68	139/74	4
DO390	-0.46236/14.25903	1805.95	1.28	0.65	178/61	143/72	6
DO391	-0.45859/14.27928	1612.04	1.15	-0.26	172/69	63/70	5
DO392	-0.44671/14.28126	1834.11	1.14	-0.04	164/80	17/85	5
DO393	-0.44260/14.26056	3679.03	1.15	-0.14	192/71	188/89	4
DO411	-0.44968/14.31503	373.91	1.09	0.24	199/41	44/64	5
DO417	-0.18465/14.44160	6250.62	1.10	0.18	74/64	348/66	4
DO429	-0.20160/14.23782	332.68	1.16	-0.25	262/47	206/52	5
DO430	-0.19884/14.25771	1772.68	1.21	-0.15	281/59	202/59	5
DO431	-0.18014/14.28115	5744.89	1.31	-0.08	280/35	133/53	4
DO433	-0.19160/14.25265	226.56	1.08	-0.05	288/40	186/40	5
DO434	-0.17853/14.23728	3869.96	1.06	-0.75	249/34	78/78	4
DO435	-0.16359/14.23914	58.03	1.15	0.38	255/57	165/57	4

DO340	-0.45857/14.29676	1650.82	1.25	0.55	246/28	223/59	4
DO372	-0.18732/14.29283	1069.69	1.09	-0.51	258/56	168/56	6
DO438	-0.12858/14.27650	4807.43	1.30	0.29	235/56	191/65	5
DO439	-0.14621/14.24885	6886.97	1.26	0.30	271/36	224/44	4
DO440	-0.15228/14.23896	7389.71	1.41	-0.01	293/61	192/62	5
DO443	-0.07457/14.25051	1353.40	1.07	-0.03	131/24	118/47	4
DO447	-0.15871/14.18695	7797.94	1.16	0.15	221/48	147/49	5
DO448	-0.23558/14.20584	2103.28	1.14	-0.52	237/45	207/63	5
DO449	-0.20279/14.20782	9958.43	1.24	-0.44	250/48	175/49	5
DO450	-0.18713/14.20475	10819.98	1.27	-0.03	265/36	248/70	4
DO451	-0.20008/14.21964	3003.29	1.15	-0.60	264/15	256/62	5
DO452	-0.25300/14.20552	222.10	1.07	-0.16	270/35	152/39	4
DO455'	-0.46247/14.13541	720.99	1.16	0.14	314/13	137/52	4
DO478	-0.50011/14.21112	809.88	1.11	0.18	204/39	167/53	6
DO479	-0.46715/14.21115	1712.59	1.13	-0.35	129/51	311/90	4
DO480	-0.48066/14.18863	7322.04	1.19	-0.21	244/3	90/7	6
DO481	-0.49540/14.11114	209.24	1.05	-0.16	195/54	30/80	4
DO436	-0.16193/14.27109	5262.71	1.18	0.16	304/41	213/41	4
DO437	-0.18967/14.27640	672.04	1.20	0.46	269/67	206/69	6
DO483	-0.49114/14.01994	1355.55	1.10	-0.49	285/61	202/61	6
DO484	-0.48964/14.01198	2646.17	1.30	0.36	244/48	201/60	4
DO485	-0.46278/14.01161	1381.26	1.10	0.15	307/50	171/59	5
DO495	-0.46196/14.11876	4230.94	1.36	0.23	222/40	218/86	5
DO498	-0.45677/14.14730	9463.61	1.16	-0.33	219/36	60/64	4
DO499	-0.48035/14.15374	4384.27	1.17	-0.35	212/44	90/49	6
DO500	-0.46513/14.17176	803.97	1.05	0.01	208/58	182/74	5
DO501	-0.44741/14.17020	4483.33	1.11	-0.04	245/38	140/39	5
DO508	-0.36310/14.13710	2287.78	1.23	0.49	48/6	31/20	5
DO518	-0.39413/14.07950	571.89	1.14	-0.22	115/41	21/41	6
DO534	-0.21632/14.15085	9758.12	1.24	-0.42	269/19	249/45	5
DO535	-0.19402/14.14965	2346.03	1.18	-0.02	270/41	251/72	4
DO536	-0.17757/14.16387	7235.33	1.20	-0.78	272/73	232/83	4
DO537	-0.16609/14.17174	5734.49	1.18	-0.70	257/60	98/78	5

Table 2

Stations	Coordinates	Scalar data			Directional data		Specimens numbers	Stations	Coordinates	Scalar data			Directional data		Specimens numbers
	Long./Lat.	Km ($x10^{-6}$)	P	T	K1	K3			Long./Lat.	Km ($x10^{-6}$)	P	T	K1	K3	
DO001	-0.02523/13.99798	931.10	1.11	0.32	50/33	280/43	4	DO030	0.01740/14.03609	897.27	1.08	0.37	68/61	285/71	5
DO002	-0.01497/14.02448	1098.11	1.17	0.07	35/72	267/76	4	DO031	0.03430/14.01497	1157.91	1.09	-0.05	16/57	312/59	6
DO003	-0.03763/13.97857	2688.42	1.10	-0.23	57/31	310/32	4	DO032	-0.01418/13.99084	503.84	1.07	0.63	87/38	324/43	6
DO004	-0.05135/13.97031	825.28	1.15	0.10	57/46	253/14	4	DO033	-0.00650/13.99144	328.18	1.05	0.35	64/47	285/59	4
DO005	-0.05272/13.95076	852.83	1.13	0.44	288/82	241/84	4	DO034	0.00017/13.97012	2728.99	1.38	0.11	188/73	115/73	5
DO009	-0.01827/14.02099	90.92	1.04	0.51	89/24	244/59	5	DO035	-0.02944/13.97024	1593.22	1.14	0.43	268/79	89/90	4
DO010	-0.00040/14.02221	819.79	1.11	0.37	99/73	292/86	5	DO036	-0.01659/13.94722	877.57	1.05	0.51	233/26	222/69	4
DO011	0.00554/14.00357	1294.86	1.11	0.15	64/73	310/74	5	DO037	-0.01561/13.93270	337.50	1.23	0.26	5/69	221/77	9
DO012	0.01755/14.02177	2596.80	1.07	0.33	61/50	278/63	5	DO038	-0.00033/13.92948	266.88	1.09	0.43	245/36	244/89	5
DO014	0.01808/14.00277	2147.36	1.12	-0.32	95/50	332/54	6	DO039	-0.00082/13.91510	1873.64	1.14	0.04	51/85	61/80	4
DO015	0.03426/14.00607	2171.55	1.07	-0.10	44/21	245/47	6	DO040	-0.05045/14.03787	442.83	1.06	-0.03	73/45	58/76	5
DO016	0.04112/13.98977	1810.73	1.08	0.16	37/11	10/34	4	DO041	0.00025/13.94904	378.82	1.09	0.38	204/82	123/82	5
DO017	0.04867/13.98536	256.74	1.05	0.42	295/6	289/42	5	DO042	0.01794/13.95267	3770.25	1.09	-0.25	326/77	257/77	5
DO018	0.05407/13.96787	5011.62	1.12	0.06	20/18	232/31	5	DO043	0.03632/13.94356	2348.22	1.19	-0.19	259/70	181/71	6
DO019	0.07034/13.96610	198.78	1.04	-0.28	259/53	139/53	6	DO044	0.03040/13.93318	1080.90	1.07	-0.25	34/82	229/88	5
DO020	0.05532/13.94726	1719.30	1.16	0.29	303/67	198/67	5	DO045	0.07948/13.98645	785.92	1.14	0.20	215/62	146/63	5
DO021	0.05229/13.93260	721.46	1.09	0.01	342/68	185/81	5	DO046	-0.05610/14.02120	475.28	1.10	0.12	49/54	262/68	5
DO022	-0.03171/13.99602	482.53	1.08	0.15	330/46	294/59	4	DO047	-0.07178/14.01784	405.75	1.08	0.69	308/35	271/47	4
DO023	0.07126/13.94896	779.14	1.09	0.54	101/64	44/68	6	DO048	-0.07314/14.00365	411.86	1.06	0.43	251/17	249/86	4
DO024	0.07069/13.93244	290.75	1.11	0.13	278/55	237/65	6	DO049	-0.05330/14.00480	2368.53	1.13	0.11	54/39	300/42	5
DO025	0.06692/13.91473	1146.05	1.13	0.49	257/54	228/72	4	DO050	-0.07530/13.96611	318.80	1.06	0.18	327/62	216/68	4
DO026	0.07567/13.89181	296.67	1.07	0.04	301/72	221/73	5	DO051	-0.07546/13.94824	989.19	1.11	0.04	28/78	1/85	4
DO027	0.04091/13.96901	1711.47	1.08	-0.15	359/67	326/86	4	DO052	-0.05883/13.98039	334.97	1.08	0.72	74/44	282/64	6

DO028	0.01777/13.96386	950.91	1.15	0.34	303/59	133/84	5
DO029	0.00223/14.04294	354.12	1.06	0.16	104/3	285/70	5
DO055	-0.01760/13.89443	1361.99	1.14	0.64	215/65	68/76	5
DO056	-0.06521/13.91495	801.37	1.07	0.16	247/74	83/85	6
DO057	-0.04443/13.94632	129.25	1.03	0.32	105/37	12/37	4
DO058	0.02740/14.03973	3320.24	1.14	-0.14	300/1	123/11	6
DO059	0.01253/14.04534	1786.21	1.15	-0.08	275/6	272/62	9
DO060	-0.02122/14.03908	1023.92	1.12	0.11	259/27	251/74	6
DO061	0.07352/14.02346	3739.33	1.14	0.41	171/87	352/90	5
DO062	0.09451/14.03167	1790.87	1.18	0.24	218/78	154/79	6
DO063	0.06633/14.02486	2148.47	1.10	0.12	178/50	175/87	6
DO064	0.10794/14.03044	1600.72	1.10	0.00	287/63	269/81	6
DO066	0.11266/14.06605	147.50	1.11	0.11	210/51	175/65	6
DO071	0.06965/14.09113	3684.96	1.13	0.32	163/79	131/84	6
DO072	0.05246/14.04600	135.41	1.06	0.48	319/12	149/50	6
DO073	0.04980/14.05506	1021.42	1.06	-0.17	278/81	102/89	6
DO074	0.05871/13.99891	3897.92	1.07	0.19	202/31	129/48	6
DO075	0.04660/13.91925	912.02	1.08	-0.35	331/67	202/72	6
DO076	0.01222/13.99012	3922.83	1.17	-0.44	45/69	302/70	4
DO077	0.03301/13.91252	893.94	1.07	0.15	81/47	333/49	4
DO078	0.08815/13.92146	6498.42	1.13	0.11	256/40	238/70	6
DO079	0.07989/13.93847	1180.42	1.12	0.24	261/33	224/47	7
DO080	0.06522/13.92921	488.35	1.07	-0.05	293/37	259/54	6
DO082	0.06790/13.88189	462.48	1.12	0.06	248/74	73/88	6
DO083	0.03380/13.89536	847.99	1.15	0.13	332/74	269/76	6
DO084	0.01842/13.93223	1839.65	1.04	-0.23	278/64	106/87	6
DO085	0.01696/13.91421	2106.66	1.05	0.17	1/71	216/79	6
DO053	-0.03772/13.90623	40.22	1.02	0.65	265/44	101/78	4
DO054	-0.03688/13.89262	100.47	1.15	0.21	93/74	86/89	4
DO088	0.02497/14.02744	1686.01	1.13	0.51	315/19	305/64	6
DO090	0.08253/14.01756	4248.03	1.13	0.06	257/77	195/79	6
DO091	0.08470/13.99618	6988.56	1.16	0.04	253/70	182/71	6
DO092	0.10469/14.00076	3739.52	1.15	-0.03	266/55	167/54	4
DO094	0.10204/13.96658	3063.87	1.20	0.02	236/35	180/41	5
DO095	0.07426/13.97378	2990.89	1.12	-0.66	237/52	71/79	5
DO101	0.10400/14.08623	2338.83	1.11	0.32	185/63	174/84	5
DO102	0.08458/14.08248	3134.64	1.08	0.26	141/31	324/85	6
DO103	0.05571/14.07456	3111.51	1.06	0.45	122/59	329/75	5
DO104	0.04893/14.07168	4798.00	1.09	0.42	2/77	309/79	6
DO105	0.08335/13.94832	576.92	1.08	0.29	257/37	218/51	4
DO106	-0.04517/14.08300	3528.33	1.13	-0.01	255/30	242/69	5
DO107	0.01354/14.11832	5485.40	1.16	0.30	267/33	264/85	5
DO108	0.01507/14.13629	1770.30	1.21	0.67	84/10	87/89	4
DO109	0.02566/14.15057	81.05	1.09	0.31	268/2	88/90	5
DO111	0.03587/14.13563	223.51	1.10	0.06	83/54	72/83	4
DO113	0.04004/14.15104	628.75	1.18	0.66	277/67	104/87	6
DO114	-0.01201/14.09189	1422.16	1.12	0.03	252/13	76/74	4
DO115	-0.06171/14.11540	64.11	1.08	0.59	227/52	62/79	5
DO150	0.08430/13.91229	296.25	1.11	0.38	283/67	271/85	5
DO161	0.04600/13.91334	585.46	1.14	0.26	316/55	250/59	4
DO165	-0.02611/13.83377	2180.42	1.09	-0.32	108/50	89/76	4
DO169	-0.02519/13.82193	560.24	1.06	0.11	93/84	278/89	6
DO171	-0.00360/13.87793	275.45	1.08	0.57	25/70	255/74	5
DO172	-0.02012/13.87783	37.14	1.07	-0.05	142/82	58/82	6

DO086	0.01948/13.89709	266.61	1.06	-0.08	124/72	0/75	6
DO087	-0.00081/13.89444	1291.30	1.13	-0.03	305/83	271/86	6
DO175	0.01817/13.85768	365.61	1.08	-0.07	77/68	54/81	6
DO176	-0.00036/13.86354	279.81	1.06	0.14	360/60	221/69	6
DO177	-0.02900/13.91264	135.07	1.08	0.18	207/69	60/78	5
DO178	-0.01572/13.86224	546.75	1.12	-0.28	119/81	74/84	5
DO181	-0.06413/13.89665	59.24	1.02	0.26	199/54	66/63	5
DO196	0.10775/13.93034	593.56	1.07	0.10	314/44	267/56	4
DO197	0.08958/13.92898	681.87	1.11	-0.01	271/50	232/62	5
DO198	0.10121/13.94968	947.92	1.08	0.46	280/24	241/35	7
DO203	0.09101/13.97033	69.63	1.25	0.63	276/40	156/44	6
DO206	-0.02392/14.08692	1304.41	1.15	0.76	247/39	239/76	4
DO207	-0.01388/14.08407	116.94	1.19	-0.34	262/21	99/52	6
DO208	0.00555/14.07442	3930.39	1.18	0.80	78/52	222/87	6
DO209	0.02352/14.07248	2375.84	1.16	0.37	270/23	220/68	5
DO211	0.04011/14.09291	6013.33	1.13	0.61	284/41	278/83	6
DO212	0.02308/14.09916	4572.72	1.16	0.51	79/58	265/86	6
DO213	0.00121/14.08803	1682.20	1.18	0.32	239/70	79/83	6
DO214	-0.03626/14.09265	436.51	1.09	0.40	271/23	99/72	6
DO215	-0.03816/14.11533	663.43	1.12	0.81	81/22	70/61	4
DO216	0.04234/14.11194	3187.80	1.11	0.49	287/28	284/84	6
DO217	0.06401/14.10577	4838.20	1.11	0.43	309/30	129/89	4
DO218	0.07608/14.10525	3389.34	1.14	0.47	284/56	137/70	7
DO173	-0.03713/13.87814	177.39	1.04	-0.08	115/32	96/62	6
DO174	0.03312/13.87783	1475.78	1.13	0.01	65/70	255/87	5
DO219	0.08777/14.11287	3543.61	1.13	0.06	131/19	314/84	4
DO223	0.07399/14.14483	119.59	1.08	0.73	115/33	115/89	6
DO224	0.05787/14.14347	755.02	1.29	0.49	258/81	92/88	5
DO225	-0.00053/14.12902	104.49	1.06	-0.22	78/2	258/80	5
DO226	0.00235/14.14417	803.11	1.13	0.64	236/24	62/78	4
DO227	-0.01211/14.12836	456.76	1.07	0.69	241/42	84/67	6
DO228	-0.04262/14.13349	116.06	1.09	0.70	86/49	65/72	5
DO230	0.03542/14.16078	52.77	1.09	0.65	285/70	269/84	6
DO238	-0.05097/14.12231	174.57	1.12	0.59	67/5	65/66	5
DO242	-0.05410/14.09787	43.59	1.03	0.32	49/42	34/75	4
DO246	-0.08973/14.00374	409.70	1.05	0.75	51/8	233/80	6
DO247	-0.10780/14.00223	231.60	1.11	-0.18	52/32	299/34	6
DO250	-0.09762/13.98769	1700.46	1.09	0.31	283/69	208/69	5
DO251	-0.09906/13.96436	2109.33	1.05	-0.24	80/65	45/77	4
DO252	-0.10885/13.97153	1034.11	1.07	-0.02	44/47	9/62	5
DO269	-0.09358/13.95135	1145.93	1.10	-0.06	283/75	190/74	5
DO270	-0.07535/13.93169	1958.65	1.07	-0.63	357/85	213/87	6
DO271	-0.06037/13.93201	161.37	1.07	0.57	260/65	226/75	5
DO274	-0.06634/13.94315	129.70	1.08	-0.20	63/51	35/69	6
DO275	-0.10178/13.97818	734.88	1.06	0.33	305/78	199/79	6

Table 3

Stations	Coordinates	Scalar data			Directional data		Specimens numbers	Stations	Coordinates	Scalar data			Directional data		Specimens numbers
	Long./Lat.	Km ($x10^{-6}$)	P	T	K1	K3			Long./Lat.	Km ($x10^{-6}$)	P	T	K1	K3	
DO120	-0.45665/14.02430	691.38	1.08	0.30	188/50	182/85	6	DO323	-0.27093/14.38664	669.83	1.11	-0.16	8/83	255/84	4
DO121	-0.47649/14.03705	4685.38	1.14	-0.23	234/48	169/50	5	DO324	-0.29485/14.38227	2167.41	1.09	0.11	235/53	113/58	4
DO137	-0.19386/14.41547	52.91	1.04	0.30	75/77	273/86	5	DO329	-0.31061/14.41130	16744.76	1.28	0.29	112/57	14/57	5
DO138	-0.21051/14.42247	32.75	1.03	-0.002	307/62	140/83	5	DO332	-0.38855/14.33392	512.07	1.07	0.21	69/61	23/68	6
DO139	-0.30539/14.39267	1558.60	1.12	0.08	146/39	88/49	4	DO333	-0.40304/14.32910	777.31	1.05	0.31	256/52	219/65	5
DO140	-0.31862/14.37563	237.89	1.04	-0.75	155/62	97/67	4	DO334	-0.40307/14.31218	668.62	1.16	-0.11	214/69	99/71	6
DO141	-0.31673/14.40180	1347.51	1.22	0.01	146/69	37/72	4	DO335	-0.40401/14.29405	3280.40	1.16	0.31	143/42	83/46	5
DO145	-0.44414/14.03425	1755.83	1.22	0.13	192/21	183/71	4	DO336	-0.38739/14.31021	7062.37	1.24	-0.67	164/50	94/51	6
DO147	-0.50124/14.07324	3501.38	1.26	0.23	241/65	212/78	4	DO337	-0.42383/14.31666	149.83	1.04	0.37	231/5	230/64	4
DO151	-0.50443/14.08664	1957.44	1.22	-0.49	233/58	203/72	6	DO338	-0.43930/14.31806	118.73	1.06	0.49	246/7	66/88	4
DO153	-0.33797/14.39358	4256.02	1.09	-0.05	318/68	265/72	5	DO341	-0.43899/14.30023	1980.99	1.30	-0.13	207/61	196/84	4
DO154	-0.35699/14.38817	74.40	1.04	0.21	62/42	54/73	4	DO342	-0.42737/14.29476	3851.61	1.13	0.52	263/78	233/81	4
DO155	-0.37346/14.37877	21.66	1.06	0.15	198/51	53/66	6	DO343	-0.38834/14.29627	96.26	1.06	0.07	286/15	147/22	5
DO308	-0.25396/14.41587	962.67	1.14	-0.63	194/68	105/68	4	DO344	-0.36572/14.29296	2217.85	1.09	-0.19	139/70	103/77	4
DO309	-0.25540/14.40510	82.47	1.05	0.52	120/76	89/83	5	DO345	-0.36440/14.30656	3647.29	1.05	-0.25	218/35	139/35	6
DO313	-0.38672/14.38817	218.27	1.03	-0.11	247/81	163/82	4	DO346	-0.36148/14.33280	514.78	1.06	0.02	242/40	220/65	5
DO314	-0.19874/14.40048	140.90	1.11	-0.29	47/73	335/74	6	DO347	-0.34751/14.32122	1787.90	1.09	0.46	143/17	97/70	4
DO315	-0.20170/14.38576	222.36	1.11	-0.19	114/81	304/88	5	DO348	-0.35172/14.30804	3052.73	1.11	-0.22	138/67	60/67	5
DO316	-0.21364/14.37944	1253.74	1.16	0.40	273/55	264/85	4	DO349	-0.34631/14.29367	2523.44	1.08	0.25	291/45	133/71	4
DO317	-0.21497/14.40148	55.02	1.04	0.60	118/60	8/62	4	DO350	-0.33422/14.29446	2327.95	1.09	0.54	245/55	102/67	5
DO318	-0.23758/14.38372	171.39	1.02	-0.07	292/8	105/80	4	DO351	-0.33237/14.31622	1338.47	1.10	0.19	248/67	120/72	5
DO319	-0.25088/14.38309	981.29	1.04	0.31	287/28	267/52	4	DO352	-0.32468/14.33000	111.89	1.02	-0.02	125/23	75/26	4
DO320	-0.23630/14.40321	130.68	1.04	0.11	217/63	33/84	4	DO353	-0.31049/14.30522	508.15	1.18	-0.04	97/78	84/87	6

DO321	-0.23321/14.37188	1281.35	1.06	-0.22	96/69	286/86	4	DO354	-0.29576/14.29058	1217.15	1.12	-0.39	210/60	88/64	5
DO322	-0.23319/14.41957	51.68	1.05	-0.32	145/59	52/60	4	DO355	-0.28790/14.31109	1851.83	1.08	0.47	108/43	64/54	4
DO356	-0.29387/14.33322	35.38	1.04	0.79	197/14	21/66	4	DO403	-0.36987/14.26436	2461.27	1.06	0.07	291/46	287/86	5
DO357	-0.27587/14.33317	307.27	1.08	0.02	246/82	99/86	4	DO404	-0.36085/14.23855	1578.04	1.08	-0.24	106/45	91/75	4
DO358	-0.27751/14.31738	1682.89	1.07	0.27	239/33	77/65	5	DO405	-0.34757/14.24239	295.81	1.03	-0.09	165/15	349/57	4
DO359	-0.28092/14.29423	658.13	1.09	-0.02	290/83	245/85	6	DO406	-0.34828/14.25821	388.41	1.07	0.26	172/47	126/56	5
DO360	-0.25041/14.30216	2703.29	1.15	0.10	240/53	169/53	4	DO407	-0.34761/14.27710	2217.47	1.11	0.13	236/64	89/75	6
DO361	-0.25429/14.31529	2030.17	1.09	0.25	213/69	70/78	4	DO408	-0.33740/14.27209	534.71	1.09	0.19	146/60	42/60	6
DO362	-0.25143/14.32793	1473.68	1.04	-0.24	268/80	268/89	4	DO409	-0.32562/14.25313	789.83	1.05	-0.02	83/49	311/57	5
DO363	-0.23999/14.32876	2019.44	1.10	-0.19	100/74	85/86	4	DO410	-0.33377/14.23612	231.78	1.04	-0.10	244/8	65/83	5
DO364	-0.23710/14.31288	637.59	1.11	-0.09	205/83	70/86	4	DO412	-0.41184/14.26464	1602.29	1.12	0.14	214/79	75/83	4
DO365	-0.23858/14.29574	7667.10	1.41	-0.19	210/71	127/71	4	DO413	-0.30991/14.23722	537.59	1.09	0.18	219/14	63/30	5
DO366	-0.21817/14.29270	4141.74	1.21	0.20	199/64	75/68	6	DO414	-0.31133/14.26800	922.47	1.06	0.12	118/56	94/75	6
DO367	-0.21805/14.30849	368.49	1.11	-0.17	269/68	263/88	4	DO415	-0.31466/14.27713	2922.46	1.14	-0.15	232/86	99/86	4
DO368	-0.21959/14.32892	3040.48	1.09	0.01	174/84	60/84	5	DO418	-0.29469/14.27927	1203.01	1.12	0.19	227/24	68/51	5
DO369	-0.19978/14.32576	11224.75	1.30	-0.002	257/64	237/81	4	DO419	-0.29319/14.26031	3330.79	1.19	0.36	165/31	121/40	5
DO370	-0.20314/14.31300	1219.88	1.11	-0.40	207/70	181/81	4	DO420	-0.29525/14.24088	226.79	1.02	0.07	178/16	169/62	6
DO371	-0.19944/14.29566	11171.63	1.13	-0.18	196/53	110/53	5	DO421	-0.27712/14.24137	612.93	1.10	0.55	168/35	125/49	4
DO374	-0.17636/14.34619	1852.15	1.17	-0.10	247/59	151/59	6	DO422	-0.27390/14.25000	437.88	1.09	0.36	242/42	304/20	4
DO375	-0.18357/14.33521	6587.96	1.44	0.02	248/51	102/66	5	DO423	-0.25626/14.27450	2316.39	1.09	0.12	207/70	100/71	5
DO394	-0.42502/14.22379	2421.57	1.07	-0.16	195/67	135/69	6	DO424	-0.25417/14.25858	629.98	1.18	-0.22	259/63	211/55	4
DO395	-0.42241/14.25863	1949.73	1.07	0.04	256/73	217/83	4	DO425	-0.25697/14.24055	1190.82	1.09	0.52	262/48	116/63	5
DO396	-0.42321/14.27749	1812.18	1.08	-0.004	227/62	58/84	5	DO426	-0.24023/14.24012	4620.55	1.39	0.17	287/43	172/46	5
DO397	-0.40587/14.27880	665.30	1.07	-0.34	16/87	285/87	5	DO427	-0.24264/14.25333	404.70	1.09	0.69	185/31	160/58	4
DO398	-0.40520/14.23614	4276.89	1.06	-0.37	223/57	136/57	5	DO428	-0.22726/14.24445	1298.12	1.15	0.13	234/75	187/79	5
DO399	-0.39049/14.24190	2059.26	1.04	0.04	238/37	92/53	5	DO453	-0.24107/14.22407	2603.72	1.19	-0.22	221/60	202/79	6
DO400	-0.38442/14.26417	1163.14	1.04	0.44	242/3	61/65	4	DO454	-0.25606/14.22213	553.85	1.03	0.25	236/42	74/61	4

DO401	-0.39131/14.28510	1531.27	1.08	0.23	152/69	106/84	6	DO461	-0.30914/14.21301	237.68	1.06	0.44	165/12	111/15	5
DO402	-0.36205/14.28438	2427.60	1.09	0.34	22/70	287/70	6	DO462	-0.31071/14.22638	170.29	1.04	0.53	220/21	127/21	5
DO463	-0.29371/14.22068	564.92	1.17	0.17	189/25	92/25	4	DO488	-0.45654/14.06713	48.77	1.10	0.34	291/31	142/51	4
DO464	-0.27662/14.22344	235.33	1.06	0.32	248/50	125/55	5	DO489	-0.44318/14.06593	877.72	1.06	0.04	192/67	167/80	5
DO465	-0.36884/14.19785	507.84	1.06	0.13	168/52	137/68	4	DO490	-0.44235/14.08114	755.01	1.05	-0.19	69/70	57/86	4
DO466	-0.35703/14.20976	195.92	1.03	0.15	154/12	347/43	5	DO492	-0.47422/14.10086	4193.28	1.35	-0.07	233/51	200/66	5
DO467	-0.33309/14.22131	133.66	1.06	0.43	177/13	100/14	4	DO493	-0.45854/14.09695	1676.99	1.13	-0.19	225/50	196/68	5
DO468	-0.39005/14.18600	1353.83	1.14	0.14	176/43	114/47	4	DO494	-0.43718/14.11780	503.49	1.09	-0.07	215/52	173/62	5
DO469	-0.40096/14.19114	646.36	1.09	0.07	241/37	120/37	4	DO496	-0.40808/14.11463	927.69	1.06	0.06	196/65	194/89	5
DO470	-0.42815/14.20458	3010.84	1.06	-0.06	193/40	67/46	5	DO502	-0.38961/14.17680	162.97	1.03	-0.21	189/56	167/75	5
DO471	-0.40674/14.20530	4674.45	1.13	-0.37	192/64	136/68	5	DO503	-0.36587/14.16332	82.90	1.04	-0.19	257/67	108/79	4
DO472	-0.38702/14.20504	645.93	1.05	-0.39	189/16	180/50	4	DO504	-0.39554/14.14187	3147.97	1.25	0.35	183/53	133/60	4
DO473	-0.33478/14.20748	1100.85	1.22	0.29	205/37	133/39	6	DO505	-0.42758/14.13407	3192.59	1.09	-0.43	198/72	180/85	4
DO474	-0.34671/14.21874	98.23	1.06	0.37	183/60	123/63	5	DO506	-0.39988/14.13235	3867.43	1.24	0.51	209/59	176/72	5
DO475	-0.37235/14.22102	2380.55	1.07	0.22	189/35	61/42	6	DO515	-0.39875/14.11500	2174.14	1.10	0.12	162/64	88/43	4
DO476	-0.38667/14.22786	1445.16	1.04	0.52	153/38	99/44	5	DO516	-0.43037/14.11583	1739.54	1.22	0.07	177/73	155/88	4
DO477	-0.40652/14.22076	3160.01	1.06	0.33	243/52	155/52	6	DO517	-0.40378/14.10403	1802.55	1.15	0.16	216/79	174/80	4
DO486	-0.48136/14.02642	1529.54	1.17	-0.37	358/81	212/85	5	DO526	-0.35748/14.16583	506.79	1.07	0.08	125/65	340/81	4

Table 4

Stations	Coordinates	Scalar data			Directional data		Specimens numbers	Stations	Coordinates	Scalar data			Directional data		Specimens numbers
	Long./Lat.	Km ($x10^{-6}$)	P	T	K1	K3			Long./Lat.	Km ($x10^{-6}$)	P	T	K1	K3	
DO123	-0.25549/14.06856	388.02	1.15	-0.19	250/82	241/87	4	DO512	-0.29499/14.13088	3325.49	1.07	-0.27	203/46	188/76	6
DO124	-0.23827/14.08255	5122.77	1.24	-0.37	277/45	210/48	6	DO513	-0.29558/14.11310	2925.62	1.14	-0.45	229/50	50/90	4
DO125	-0.25882/14.09213	3827.61	1.34	-0.43	256/52	246/83	6	DO514	-0.32133/14.11722	751.96	1.19	0.74	287/31	153/43	4
DO126	-0.26163/14.11506	697.29	1.10	0.34	258/53	215/63	5	DO519	-0.33779/14.10017	239.04	1.04	0.28	200/6	185/21	5
DO127	-0.27890/14.11911	3337.77	1.10	-0.34	228/41	79/60	5	DO520	-0.31683/14.08881	1697.35	1.32	-0.11	207/32	129/33	5
DO128	-0.28129/14.13440	315.58	1.10	-0.07	182/25	114/27	5	DO521	-0.29701/14.09828	1390.78	1.15	0.40	206/20	178/32	4
DO129	-0.28779/14.10504	808.32	1.24	0.08	221/49	88/57	5	DO522	-0.29828/14.07699	2949.61	1.18	-0.26	200/60	132/62	5
DO130	-0.28114/14.09103	968.71	1.18	-0.29	247/49	244/87	8	DO523	-0.31533/14.08166	757.41	1.15	-0.05	229/46	143/46	6
DO131	-0.28008/14.07586	5855.11	1.23	-0.09	184/29	135/56	6	DO524	-0.29379/14.15147	1579.64	1.15	0.28	174/12	161/44	5
DO143	-0.24217/14.12692	4773.21	1.22	-0.31	263/52	173/52	4	DO525	-0.32659/14.14559	338.19	1.11	0.17	198/27	151/34	5
DO457	-0.23822/14.18312	5729.61	1.19	0.20	232/50	157/50	4	DO527	-0.29153/14.16745	867.94	1.14	-0.10	207/42	119/41	5
DO458	-0.25668/14.18124	1000.73	1.16	0.09	221/50	182/62	6	DO528	-0.27722/14.17038	1553.33	1.18	-0.15	225/36	171/42	5
DO459	-0.28048/14.18245	300.20	1.08	0.12	228/34	197/52	5	DO529	-0.27863/14.14897	1345.39	1.11	-0.23	193/39	110/42	4
DO460	-0.28977/14.17731	596.70	1.11	0.02	217/46	149/49	4	DO530	-0.26327/14.15254	4654.68	1.22	0.25	201/22	186/58	5
DO509	-0.33228/14.11487	230.75	1.03	0.41	256/51	166/51	6	DO531	-0.25906/14.16550	436.28	1.05	-0.26	270/31	114/56	4
DO510	-0.32807/14.12968	417.09	1.10	0.67	216/42	147/44	5	DO532	-0.24305/14.16424	8584.10	1.25	0.16	231/30	173/34	4
DO511	-0.31142/14.13535	2402.77	1.05	0.32	266/12	113/24	4	DO533	-0.23953/14.15056	775.88	1.16	0.11	263/45	200/47	4

N.B: Km in 10^{-6} SI. Km, P and T are dimensionless in the international system. K1 and K3 are given in degrees

Figures captions

Figure 1: Geological map of the Man/Léo shield

Figure 2: Location of the studied area on the synthetic geological map of Burkina Faso (modified from Castaing et al., 2003)

Figure 3: Interpretative map of the aeromagnetic image of the studied area (BUMIGEB. 2015)

Figure 4: Map of magnetic susceptibility and frequency histograms

Figure 5: Susceptibility (K) vs. Temperature (T) curves of samples of the TTG country rock and biotite granites

Figure 6: Map of shape factor (T) in the three plutons

Figure 7: Map of anisotropy degree (P) in the three plutons

Figure 8: Shape factor (T) vs. anisotropy degree (P)

Figure 9: Magnetic lineation of the Dori pluton and his country rock. (a) Organization of lineation on the map. (b) Lower hemisphere equal-area projection diagram of the lineation of Dori pluton

Figure 10: Magnetic lineation of the Gorom-Gorom and Touka Bayèl plutons and their close country rocks. (a) Organization of lineation on map view. (b and c) Lower hemisphere equal-area projection diagram of the lineation of the sector A and B of the Gorom-Gorom pluton. (d) Lower hemisphere equal-area projection diagram of the lineation of the Touka Bayèl pluton

Figure 11: Magnetic foliations of the Dori pluton and his country rock. (a) Organization of foliations on the map. (b) Lower hemisphere equal-area projection diagram of the foliations of Dori pluton

Figure 12: Magnetic foliations of the Gorom-Gorom and Touka Bayèl plutons and their close country rocks. (a) Organization of foliations on the map. (b, c, d and e) Lower hemisphere equal-area projection diagram of the foliations of the sector A. B1. B2 and B3

of the Gorom-Gorom pluton. (f) Lower hemisphere equal-area projection diagram of the foliation of the Touka Bayèl pluton

Figure 13: Main microstructures of the biotite granites and their nearby host rocks. (a) Magmatic microstructure in biotite granites. (b) Magmatic microstructure in the TTG host rock. (c) High temperature solid state deformation microstructure in biotite granite. (d) Low temperature solid state deformation microstructure in biotite granite. Hb: Hornblende – Bi: Biotite – Ep: Epidote – Pl: Plagioclase – Op: Opaque – Qz: Quartz – Mi: Microcline

Figure 14: Map of the microstructures of the three plutons. (a) Dori pluton and his nearby country rocks. (b) Gorom-Gorom and Touka Bayèl plutons and their nearby country rocks

Figure 15: Conceptual emplacement models of Gorom-Gorom (a), Touka Bayèl (b), Dori (c)

Figure 1

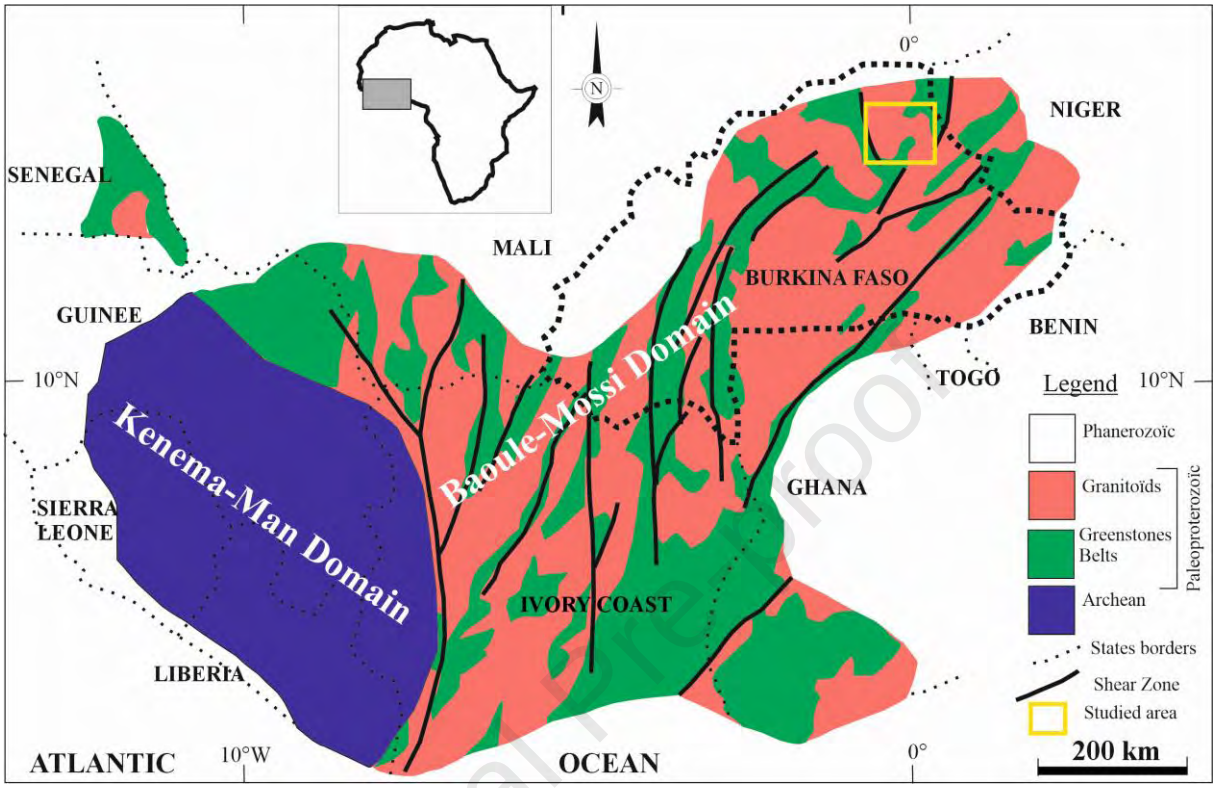

Figure 2

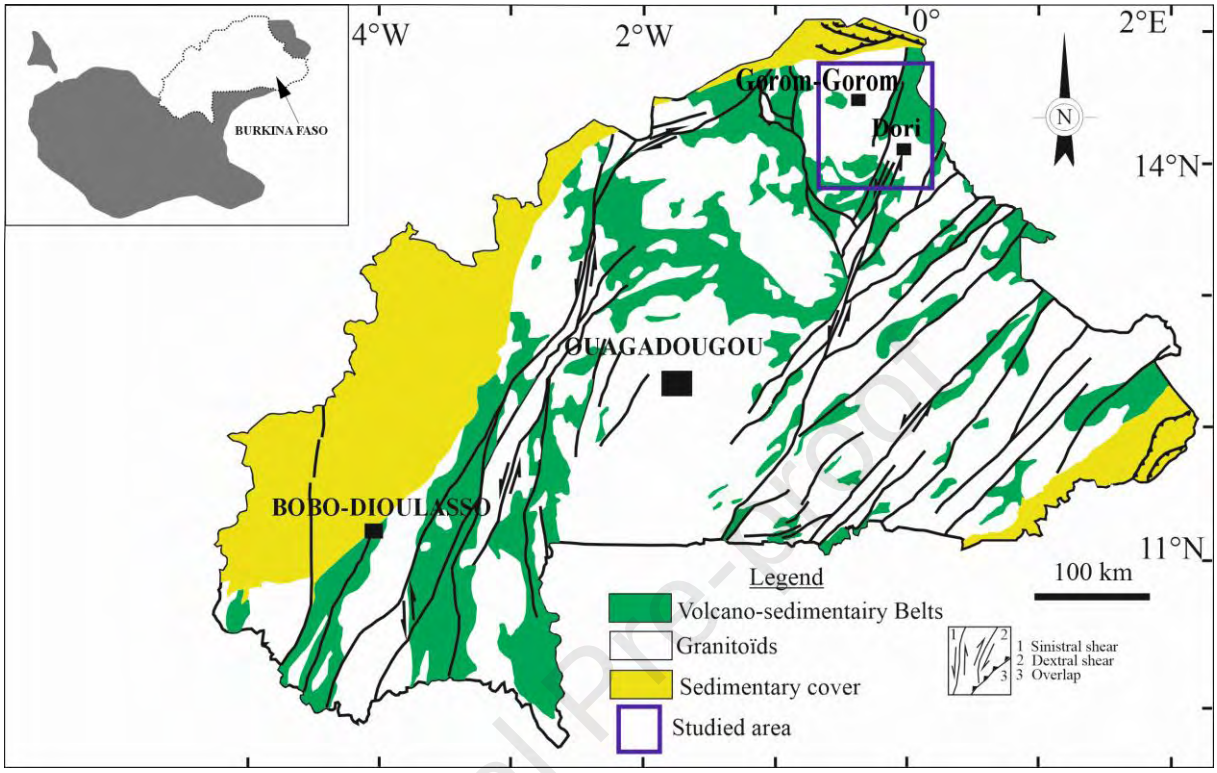

Figure 3

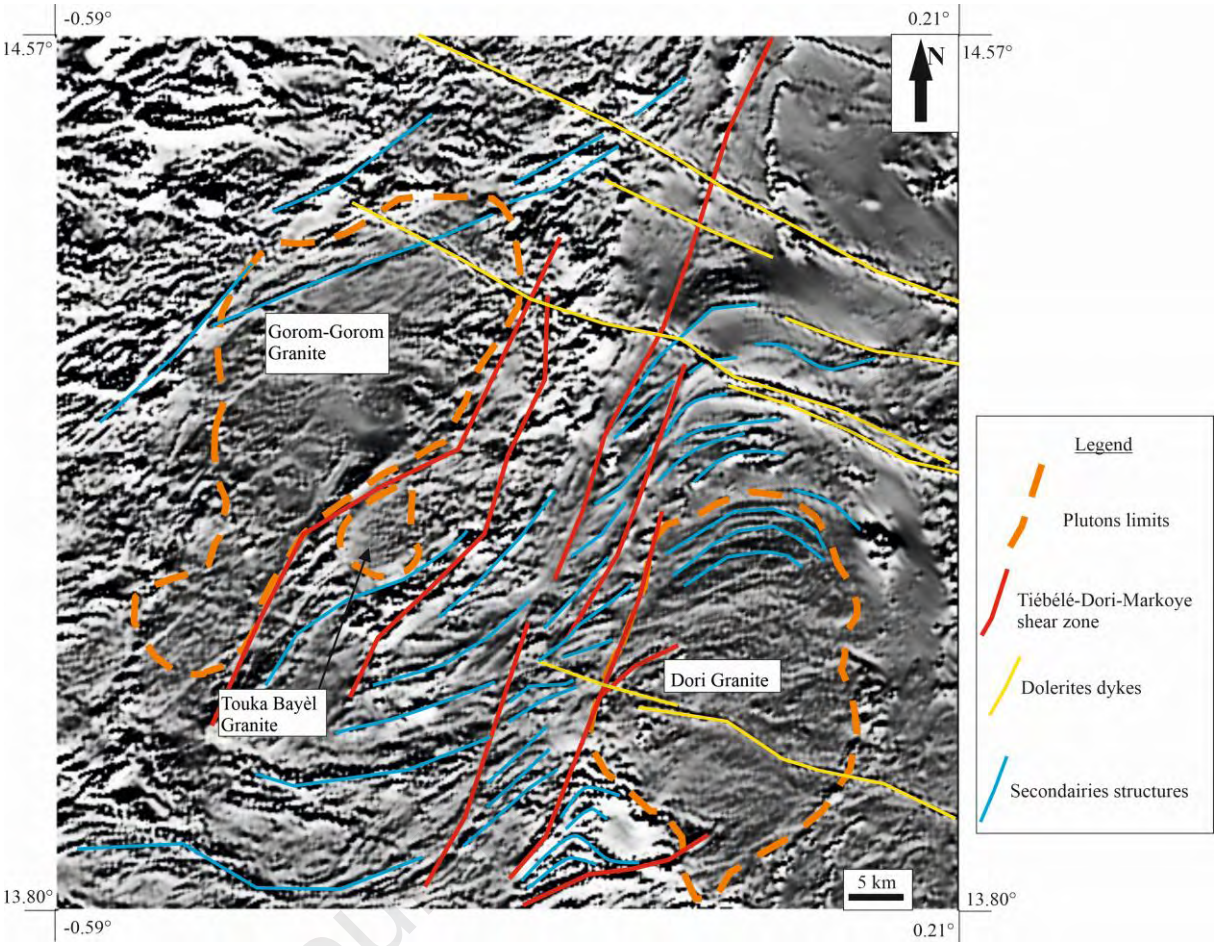
-0.59°
0.21°
14.57°
14.57°
N
Gorom-Gorom Granite
Touka Bayèl Granite
Dori Granite
Legend
Plutons limits
Tiébélé-Dori-Markoye shear zone
Dolerites dykes
Secondairies structures
5 km
13.80°
13.80°
-0.59°
0.21°

Figure 4

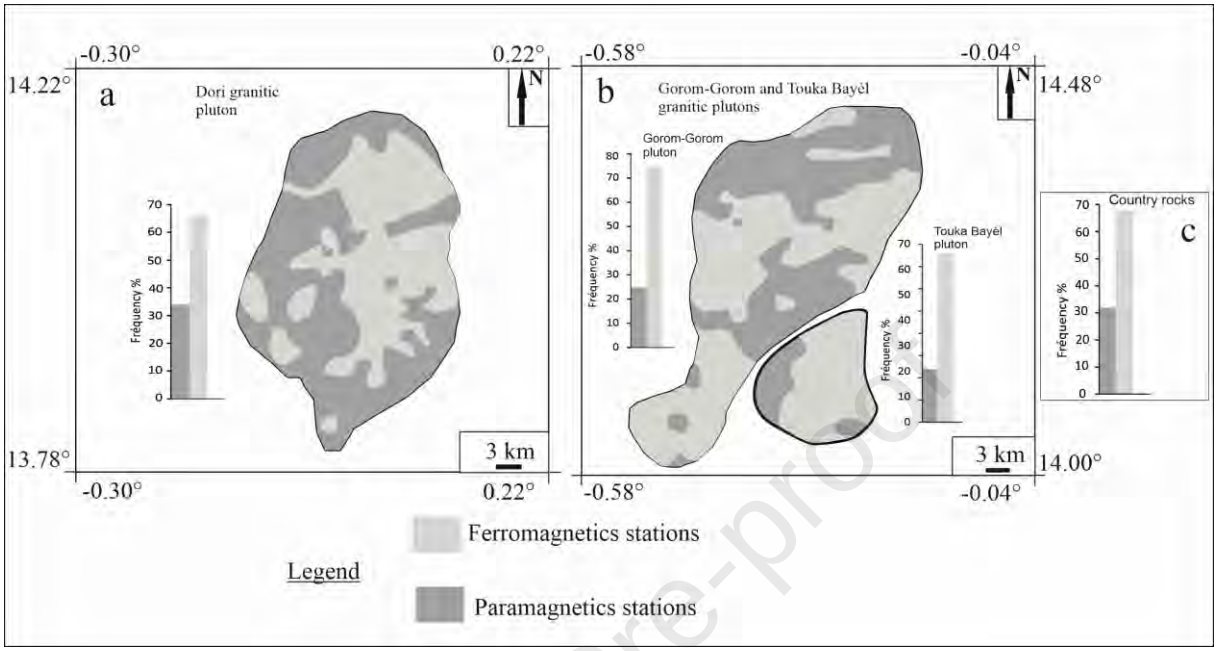

Figure 5

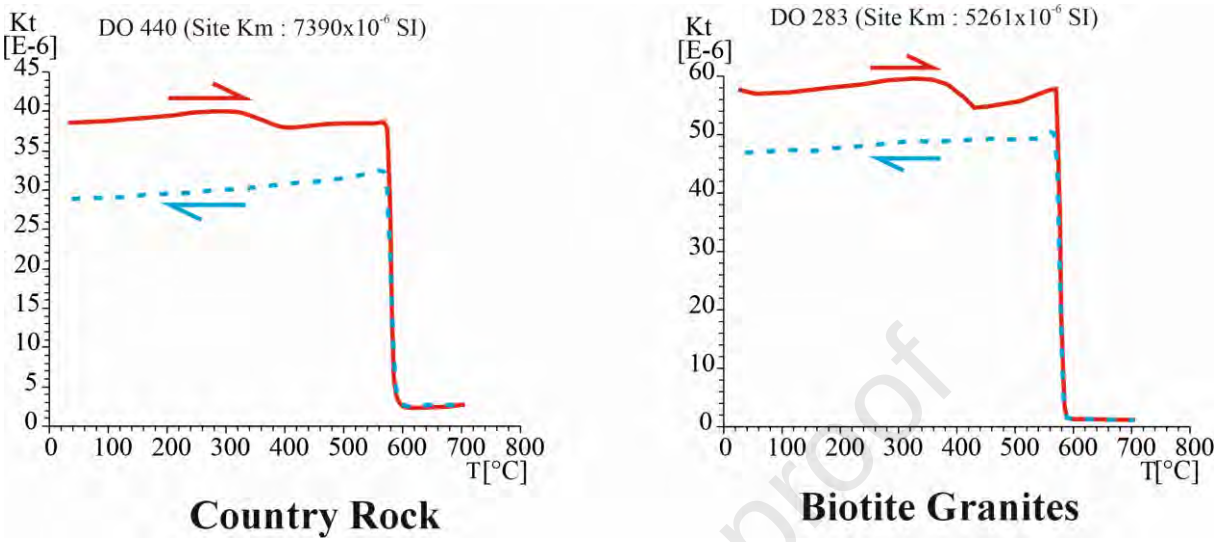

Figure 6

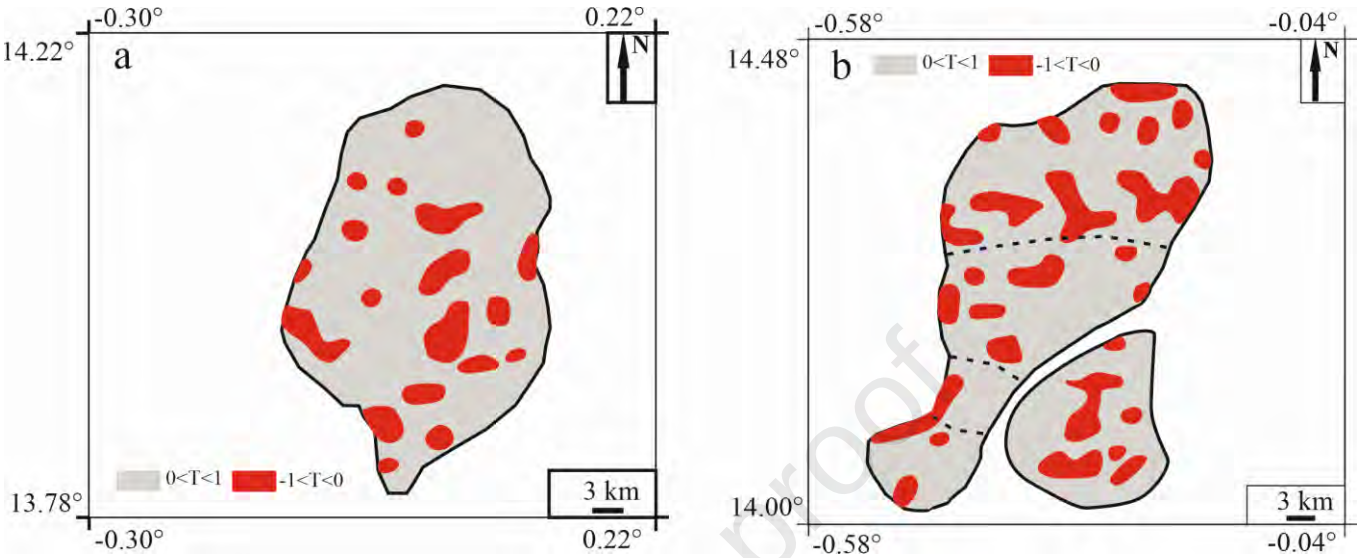

Figure 7

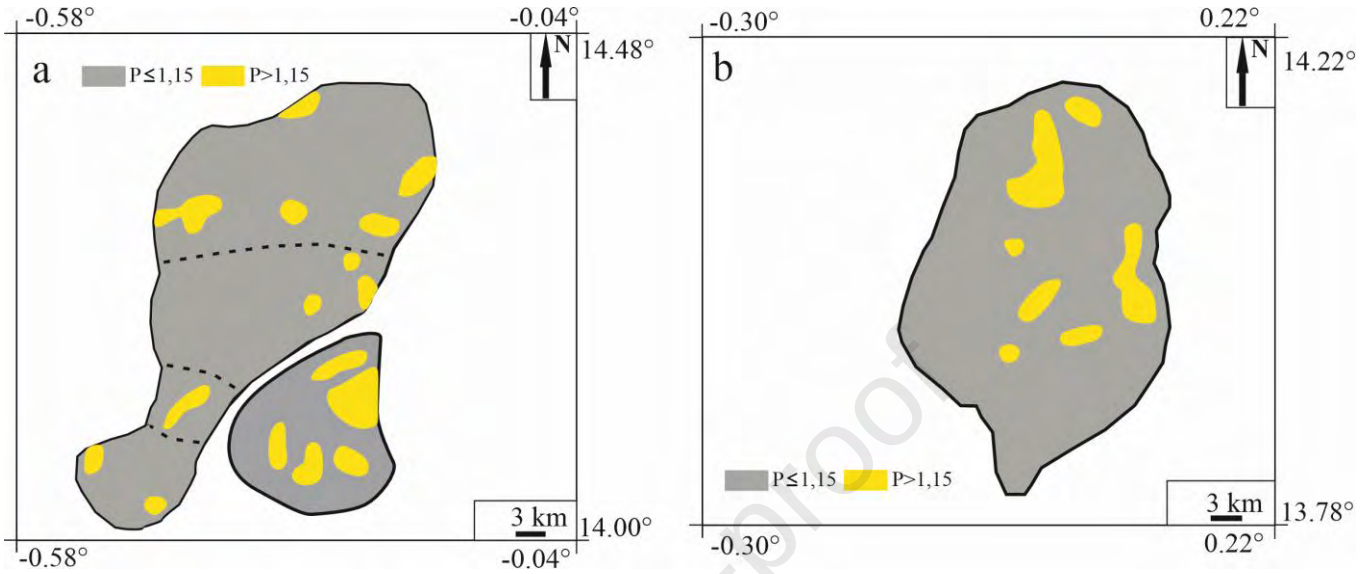

Figure 8

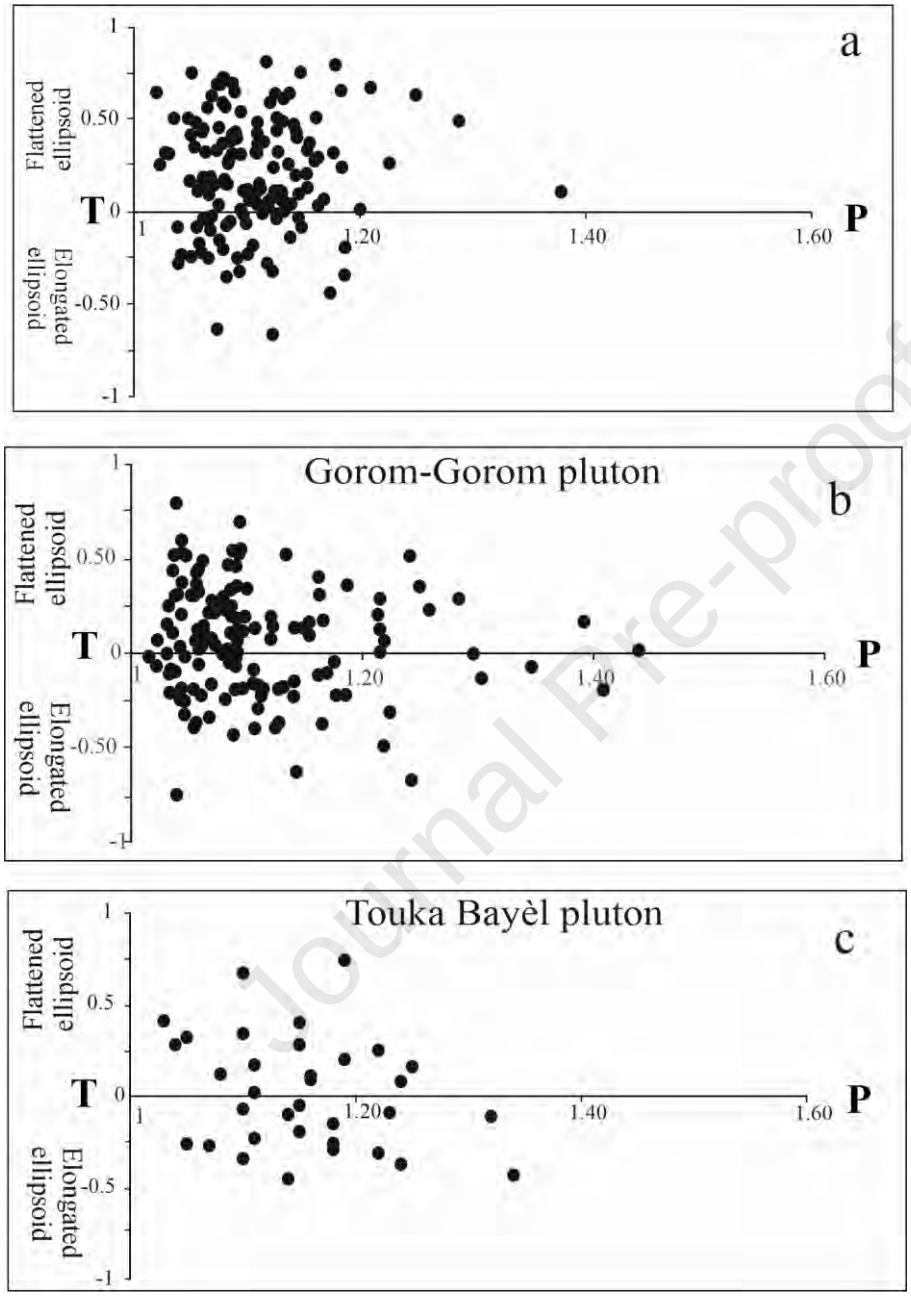

Figure 9

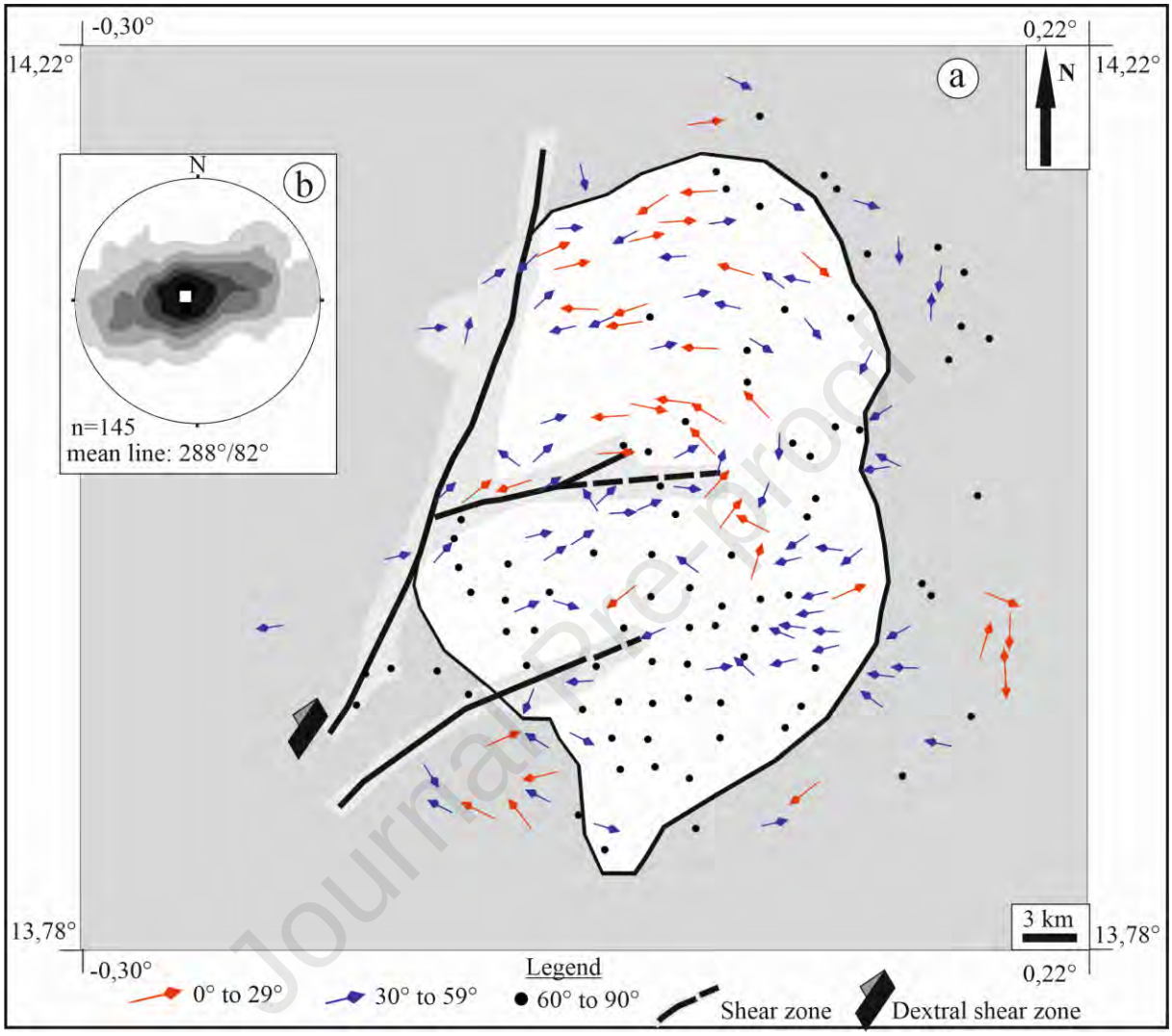

Figure 10

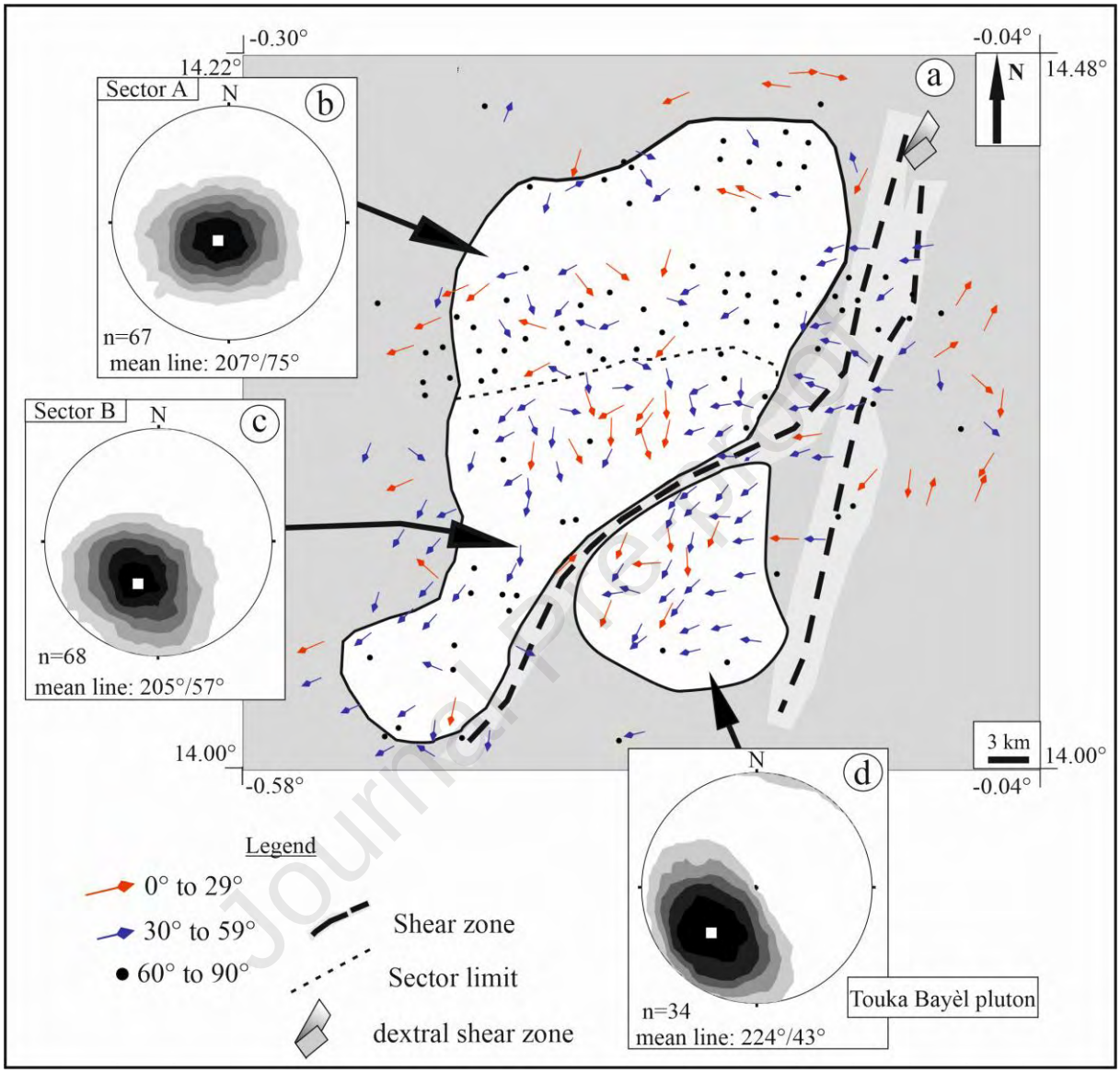

Figure 11

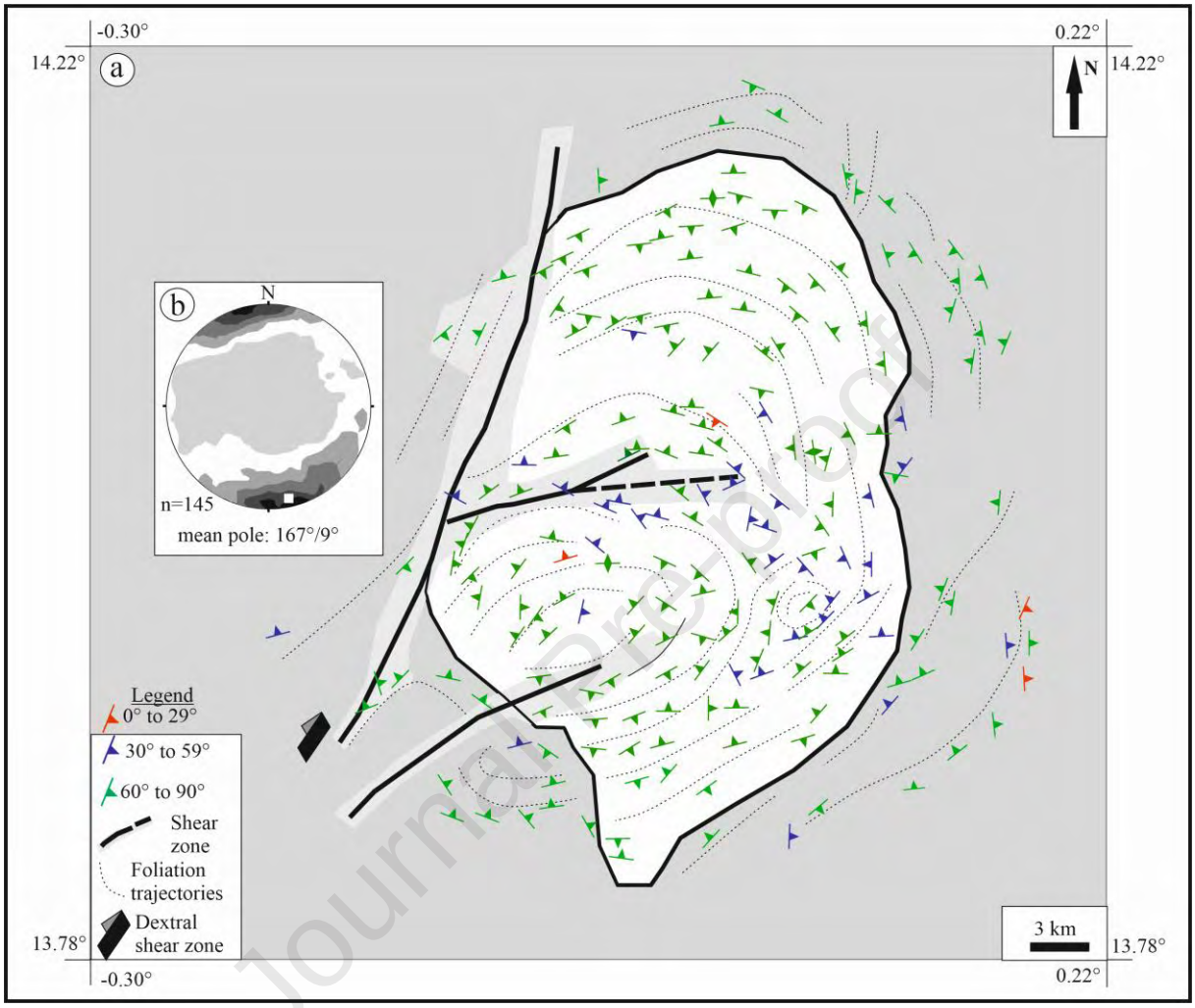

Figure 12

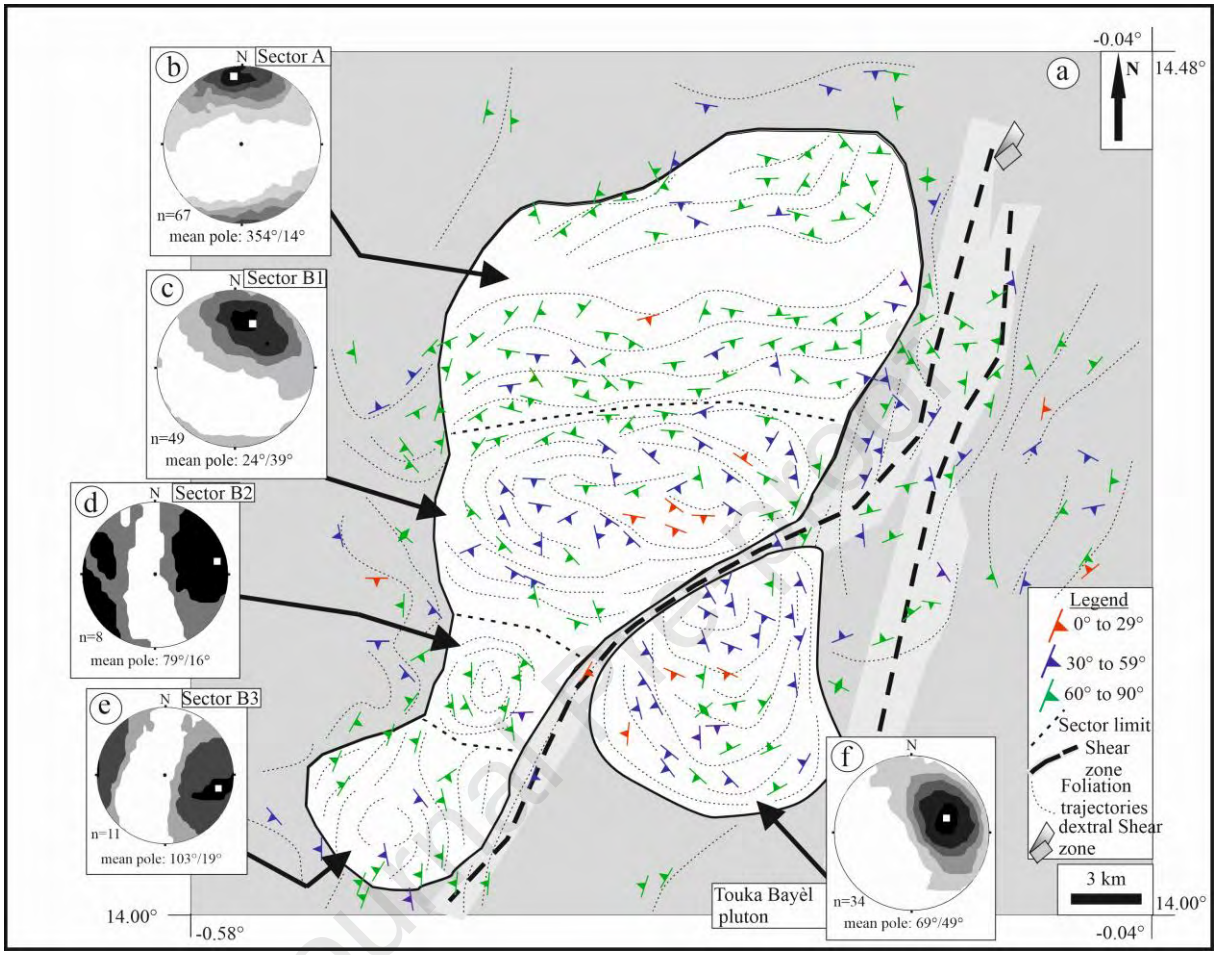

Figure 13

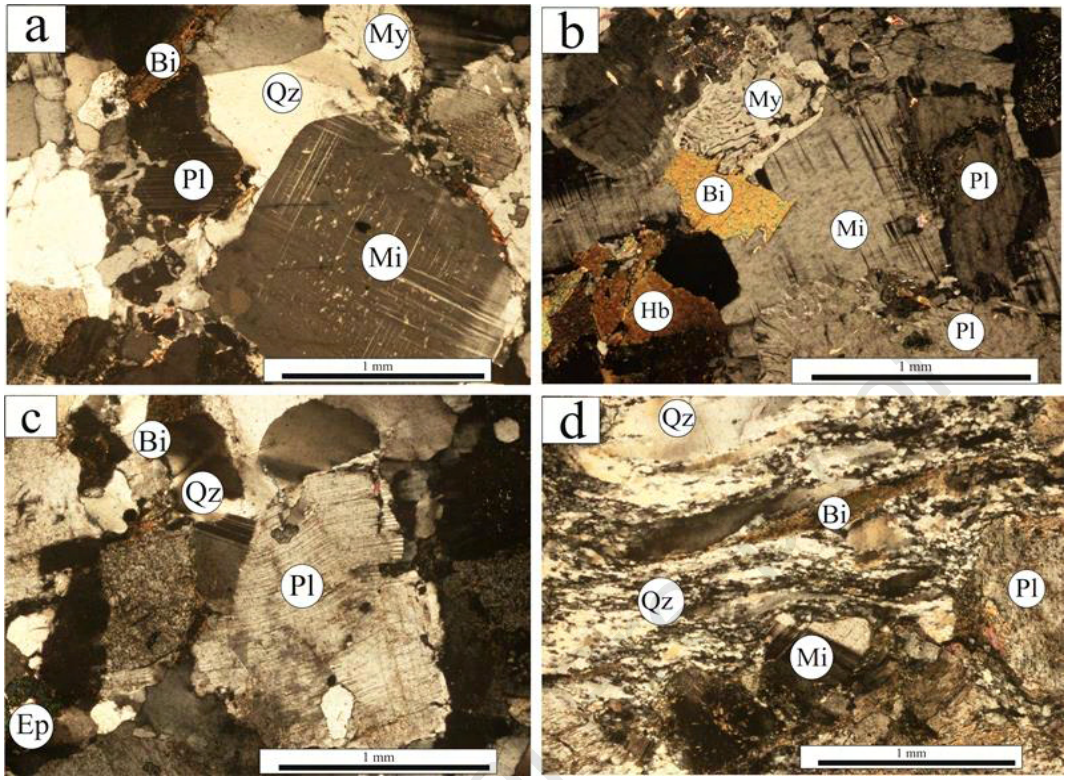

Figure 14

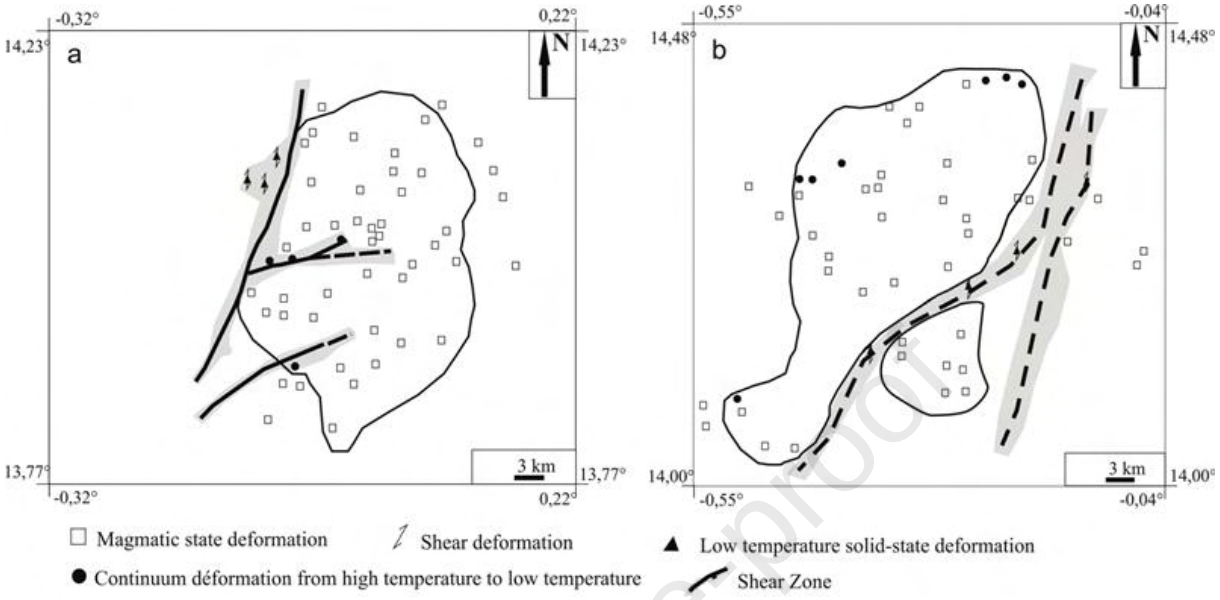

Figure 15

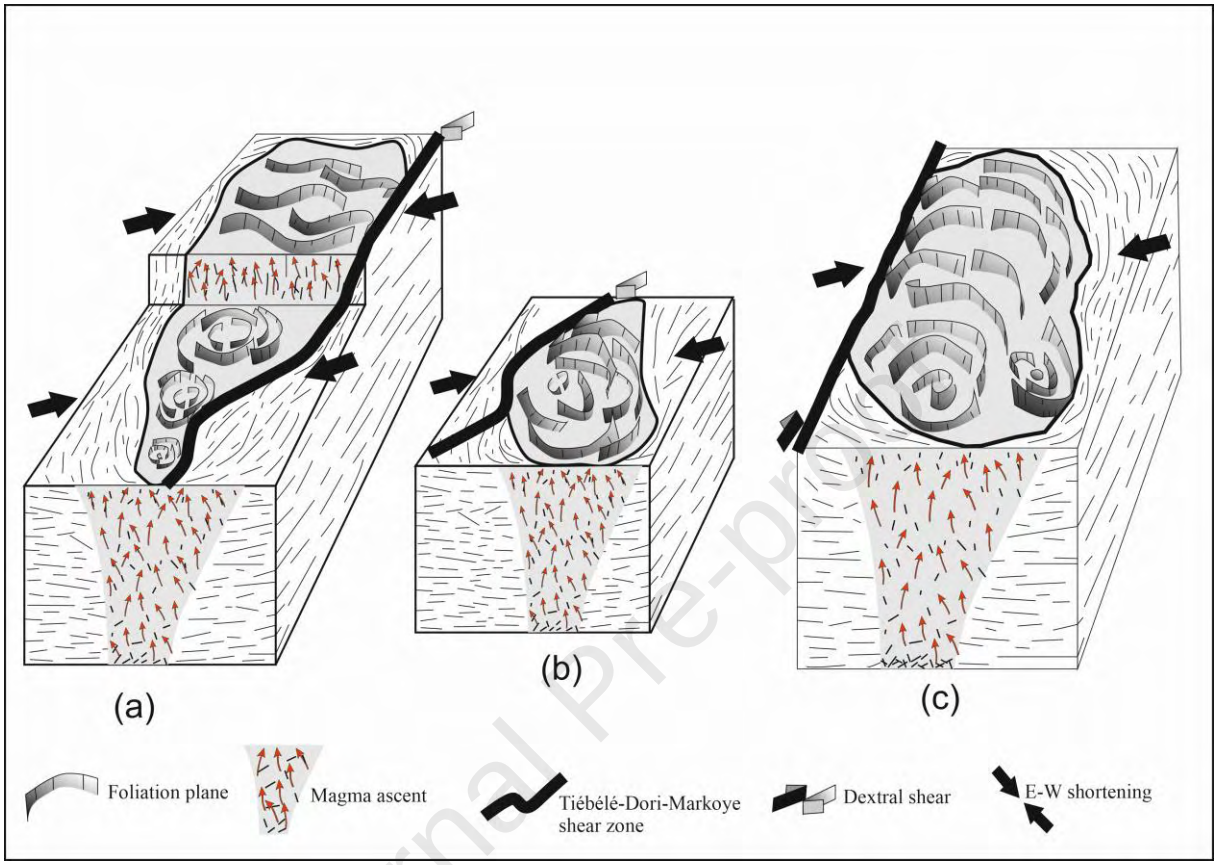

Appendix:

Appendix 1: Host rocks stereograms with K1, K2 and K3 and their limit of confidence

Appendix 2: Dori pluton stereograms with K1, K2 and K3 and their limit of confidence

Appendix 3: Gorom-Gorom pluton stereograms with K1, K2 and K3 and their limit of confidence

Appendix 4: Touka Bayèl pluton stereograms with K1, K2 and K3 and their limit of confidence

Appendix 1

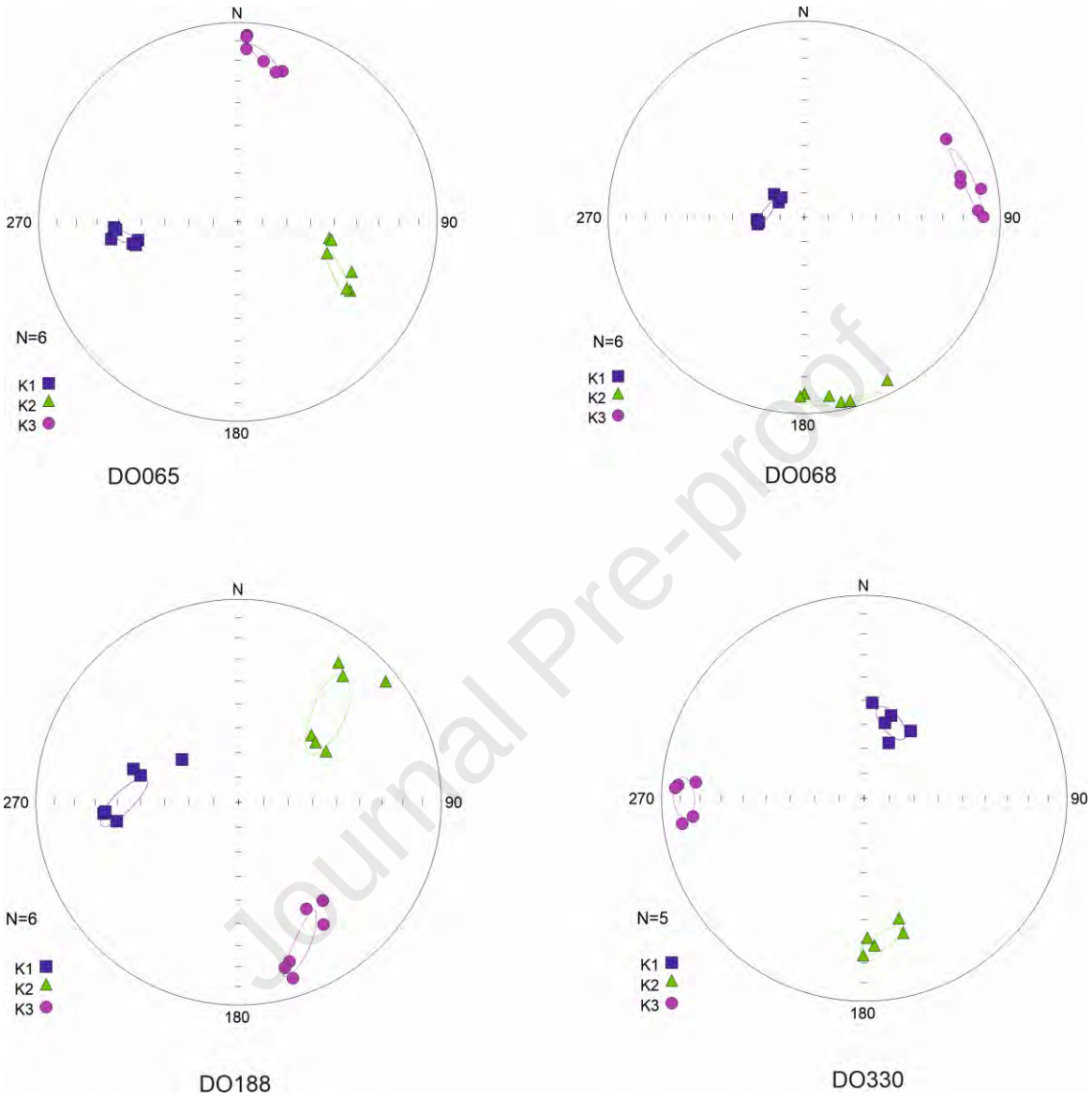

Appendix 2

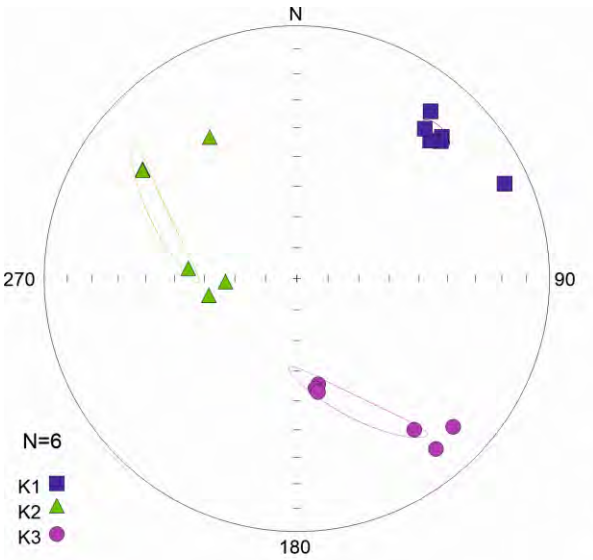

DO015

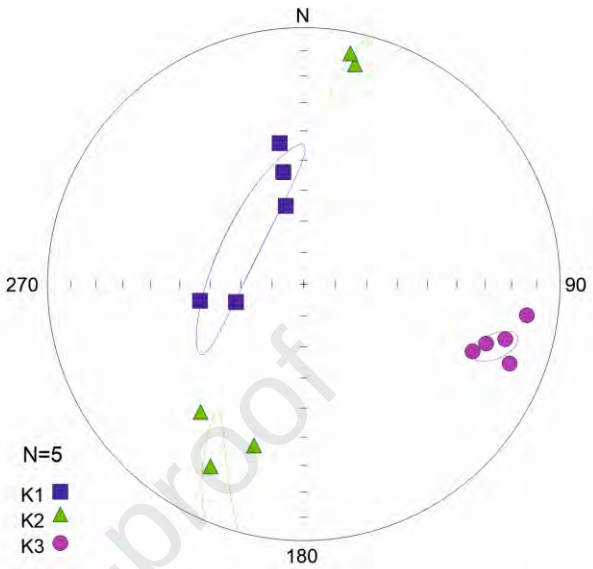

DO020

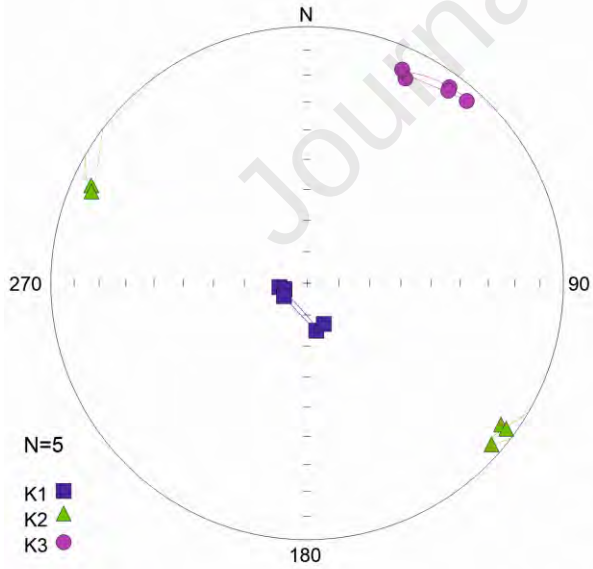

DO041

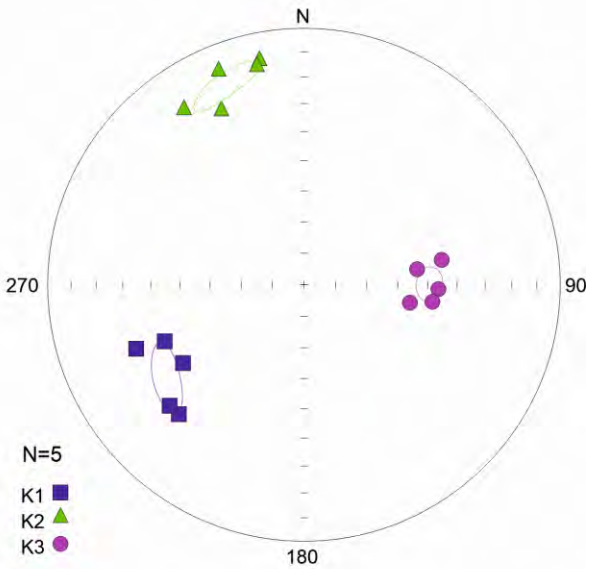

DO094

Appendix 3

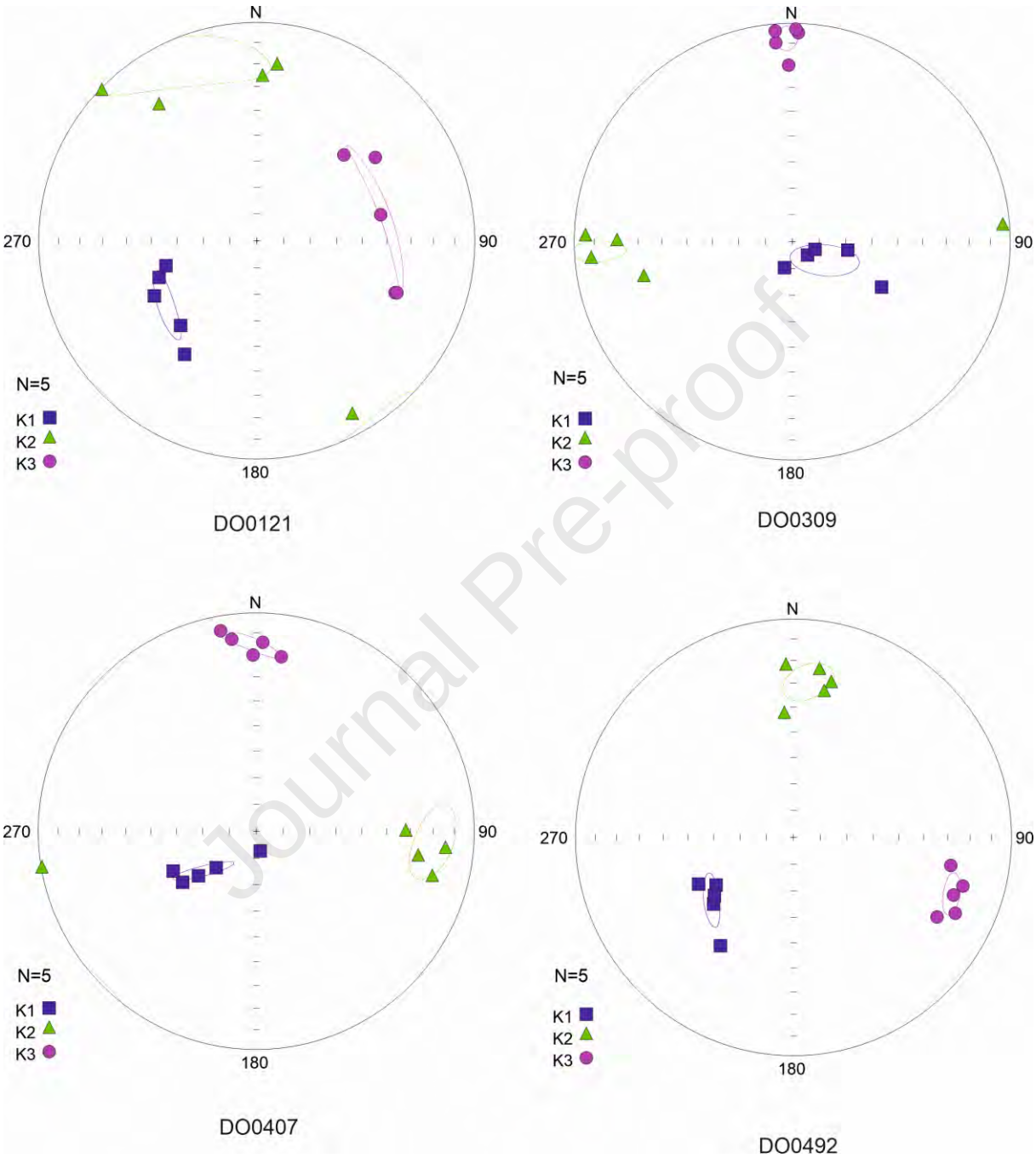

Appendix 4

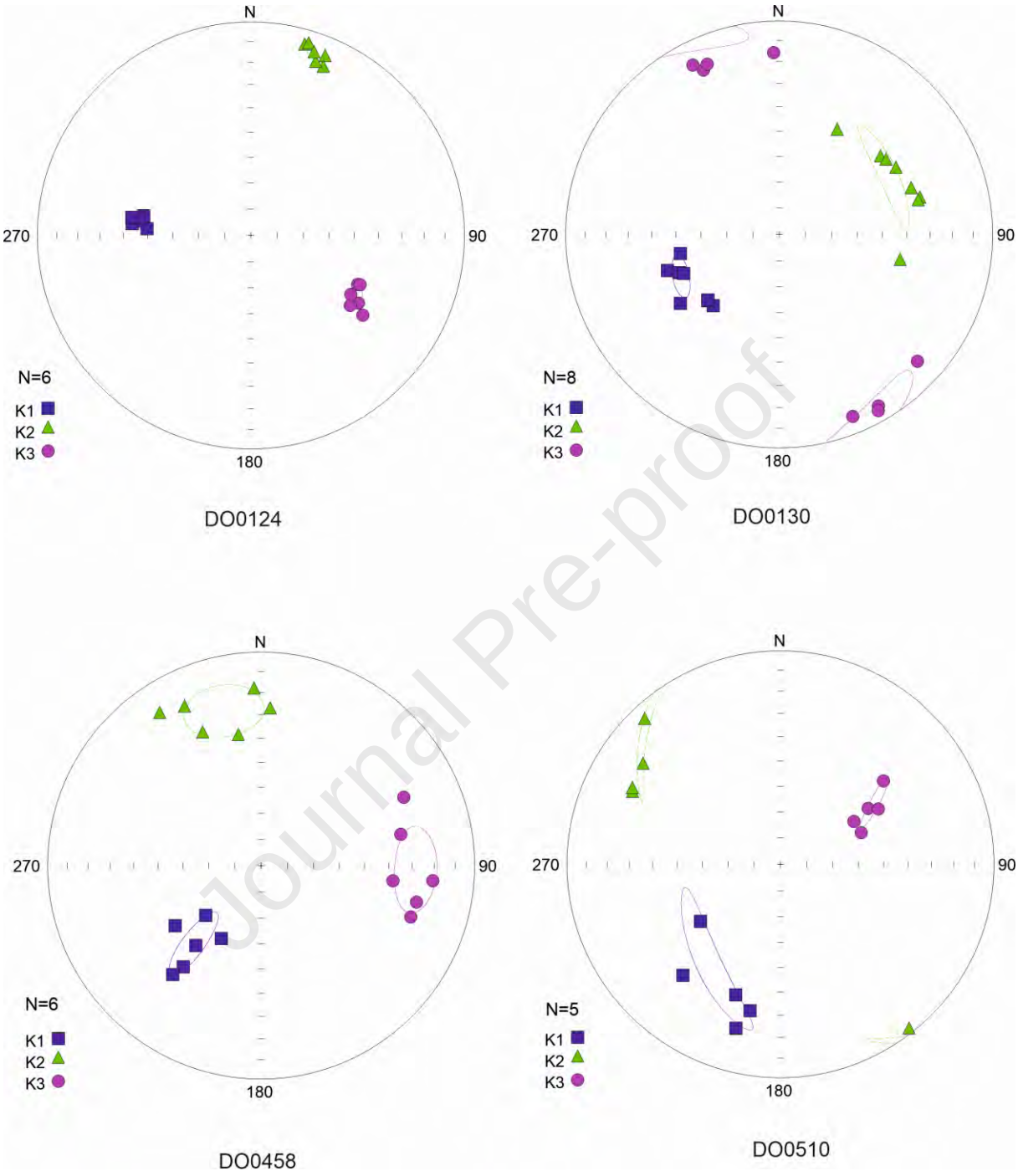

Highlights

The present paper deals with internal structures of granitic plutons which are apparently isotropic at field scale using the technique of Anisotropy of Magnetic Susceptibility (AMS) and the examination of the microstructures.

This study is going to help to reconstitute the rheological context of emplacement of these plutons. It is also going to help reconstitute the orientation of stresses which prevailed at this moment and after as the granitoid are the best markers of crustal evolution.

Declaration of interests

☐ The authors declare that they have no known competing financial interests or personal relationships that could have appeared to influence the work reported in this paper.

☒ The authors declare the following financial interests/personal relationships which may be considered as potential competing interests:

YAMEOGO reports financial support was provided by WAXI2 Programm. YAMEOGO reports equipment, drugs, or supplies was provided by Institut de Recherche pour le Développement (IRD).